The British Association of Gynaecological Pathologists

Masterclass with the Experts in Collaboration with ISGyP
4th June 2025

- What's new in gynae pathology – rounding up the literature
- Carlos Parra-Herran MD
- Brigham and Women's Hospital, Boston MA United States
- June 4th, 2025

The British Association of Gynaecological Pathologists

Speaker disclosures

Choose one

- ❑ I have no financial conflicts of interest to disclose

Lower genital squamous neoplasia

- Vulvar pathology preceding diagnosis of vulvar SCC

Gynecol Oncol 2025;192:163-170

- Concurrent *TP53* mutations and *CCDN1* gain in vulvar SCC

Mod Pathol 37 (2024) 100574

BACK

Prevalence and impact of vulvar lesions diagnosed prior to vulvar squamous cell carcinoma: A population-based cohort study

Féline O. Voss [a,b], Guus Fons [c], Annette H. Bruggink [d], Hans H.B. Wenzel [e], Johannes Berkho
Marc van Beurden [g], Maaike C.G. Bleeker [a,b,*]

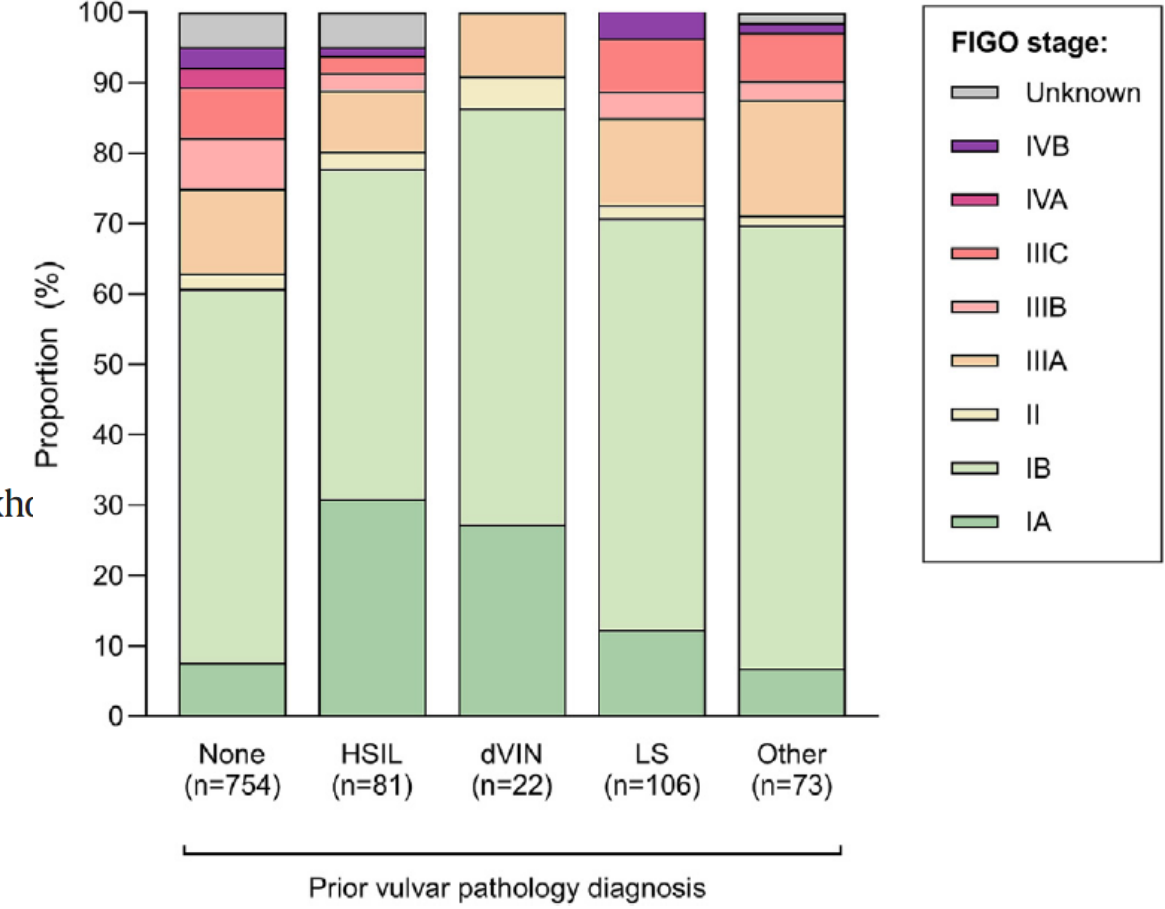

Results. A total of 1036 VSCC patients were identified, of whom most (73 %) had no prior biopsy-confirmed vulvar pathology. High-grade squamous intraepithelial lesion (HSIL) and differentiated vulvar intraepithelial neoplasia (dVIN) were diagnosed prior to VSCC in only 8 % and 2 % of cancer patients, respectively, while adjacent HSIL and adjacent dVIN were reported in 35 % and 22 % of surgical VSCC resection specimens, respectively. The remaining 17 % had a benign vulvar pathology diagnosis prior to cancer. Patients showed advanced staged tumors in 15 % and 9 % of patients with prior HSIL and dVIN, respectively, as compared to 32 % in patients without prior vulvar pathology ($p < 0.001$). There was no independent association between prior vulvar pathology and survival outcomes.

Whole-Exome Sequencing of Vulvar Squamous Cell Carcinomas Reveals an Impaired Prognosis in Patients With *TP53* Mutations and Concurrent *CCND1* Gains

Oriol Ordi[a,b], Adela Saco[b,c], Núria Peñuelas[b], Odei Blanco-Irazuegui[a], Marta del Pino[b,d], Núria Carreras-Dieguez[d], Lorena Marimon[a,c], Maria Teresa Rodrigo-Calvo[c], Alba Morató[a,b], Lia Sisuashvili[c], Mariona Bustamante[a], Adrià Cruells[a], Katarzyna Darecka[c], Naiara Vega[c], Silvia Alós[c], Isabel Trias[c], Pere Fusté[d], Genis Parra[e,f], Marta Gut[e,f], Meritxell Munmany[d], Aureli Torné[d], Pedro Jares[c], Natalia Rakislova[a,b,c,*]

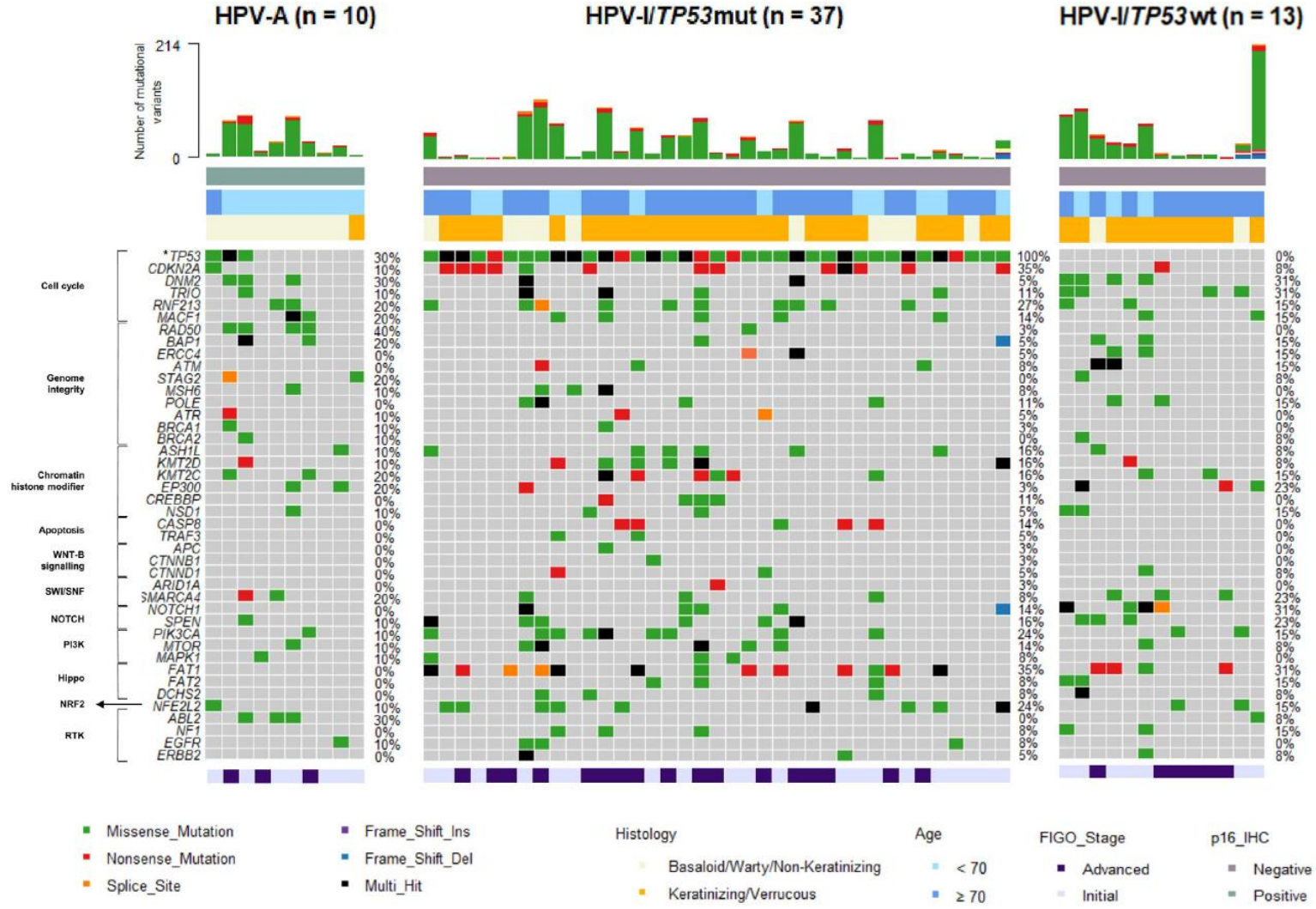

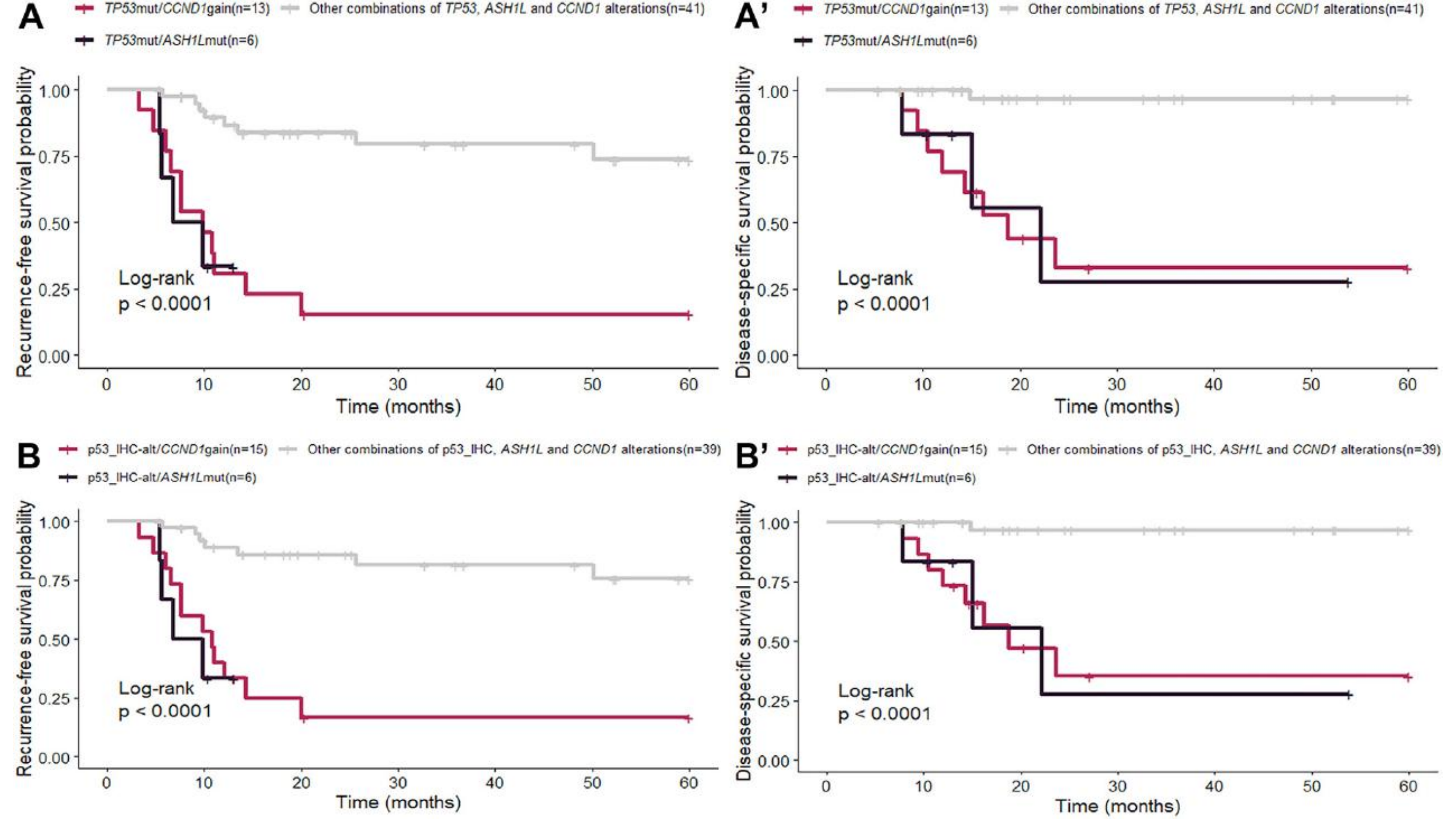
A
TP53mut/CCND1gain(n=13)
Other combinations of TP53, ASH1L and CCND1 alterations(n=41)
TP53mut/ASH1Lmut(n=6)
Recurrence-free survival probability
1.00
0.75
0.50
0.25
0.00
Log-rank
p < 0.0001
0
10
20
30
40
50
60
Time (months)
A'
TP53mut/CCND1gain(n=13)
Other combinations of TP53, ASH1L and CCND1 alterations(n=41)
TP53mut/ASH1Lmut(n=6)
Disease-specific survival probability
1.00
0.75
0.50
0.25
0.00
Log-rank
p < 0.0001
0
10
20
30
40
50
60
Time (months)
B
p53_IHC-alt/CCND1gain(n=15)
Other combinations of p53_IHC, ASH1L and CCND1 alterations(n=39)
p53_IHC-alt/ASH1Lmut(n=6)
Recurrence-free survival probability
1.00
0.75
0.50
0.25
0.00
Log-rank
p < 0.0001
0
10
20
30
40
50
60
Time (months)
B'
p53_IHC-alt/CCND1gain(n=15)
Other combinations of p53_IHC, ASH1L and CCND1 alterations(n=39)
p53_IHC-alt/ASH1Lmut(n=6)
Disease-specific survival probability
1.00
0.75
0.50
0.25
0.00
Log-rank
p < 0.0001
0
10
20
30
40
50
60
Time (months)

Lower genital squamous neoplasia

- HPV-independent SCC of the cervix associated with uterine prolapse

Int J Gynecol Pathol 2025;44:2–14

- Cervical and vulvar SCC associated with low-risk HPV

Am J Surg Pathol 2025;49:458–470

BACK

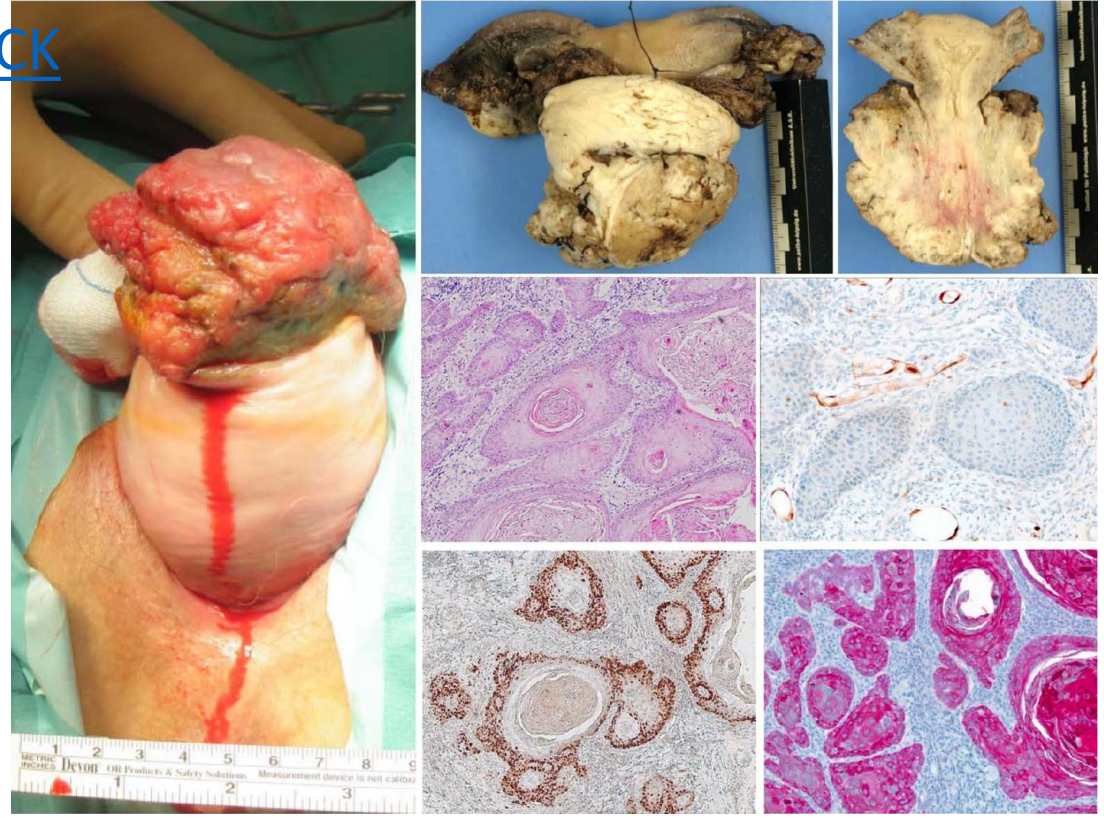

Human Papilloma Virus–Independent/p53abnormal Keratinizing Squamous Cell Carcinoma of the Uterine Cervix Associated With Uterine Prolapse

Lars-Christian Horn, MD, PhD, Christine E. Brambs, PhD,† Bahriye Aktas, PhD,‡ Astrid Dannenmann, MD,§ Jens Einenkel, PhD,§ Michael Höckel, PhD,‡ Irene Krücken, MD,*‖ Sabine Taubenheim, MD,¶ Gero Teichmann, MD,# Ulrike Obeck, MD,‖ Mathias Stiller, MD,‖ and Anne Kathrin Höhn, MD**

TABLE 1. Clinicopathologic Characteristics of SCCs of the Uterine Cervix Associated With Uterine Prolapse

Case-number	Age (yr)	Menopausal age/uterine prolapse	Tumor size	Tumor stage	p53 mutation	Treatment	Follow-up
Case #1	83	NN/NN	8.5 cm	pT2b pNX L0	c.839 G>A (p.[R280K]) exon 8, missense AF 12%, D 1030	TAH and BSO no adjuvant TX	Died 4 mon. non-tumor related
Case #2	78	50/8 yr	9.4 cm	pT4 pN1 (4/47) L1	c.742 C>T (p. (R248W)) exon 7, missense AF 46%, D 2160	LEER pelvic LNE	DOD 14 mo
Case #3	70	45/long-standing	6.0 cm	FIGO IIB, pN1 (3/30) L1	c.586 C>T (p.[R196Ter]) exon 6, stop codon AF 25%, D 1804	Pelvic LNE, radiation	Cutaneous vulval metastases 3 mo DOD 4 mo
Case #4	69	52/>2 yr	5.2 cm	pT2a2 pN0 (0/57) L1	c.1045 G>T (p.[E349Ter]) exon 10, stop codon AF 44%, D 1396	TMMR pelvic LNE	NED 20 mo

AF indicates allelic frequency; BSO, bilateral salpingo-oophorectomy; D, read depth; DOD, died of the disease; LEER, lateral extended endopelvic resection; LNE, lymphonodectomy; NED, no evidence of the disease; NN, not known; SCC, squamous cell carcinoma; TAH, total abdominal hysterectomy; TMMR, total mesometrial resection; TX, treatment.

Clinicopathologic Features and Viral Status of Low-risk HPV6 and HPV11-Associated Squamous Cell Carcinoma of the Uterine Cervix and Vulva

Guy A. Williams II, MD, Annie A. Wu, MD, PhD,* Henrietta C. Eugene, MS,* Ya-Chea Tsai, MS,* Margaret Wong, MS,* Hiro Nonogaki, MS,* Richard B.S. Roden, PhD,*†‡ Chien-Fu Hung, PhD,*† Tzyy-Choou Wu, MD, PhD,*†‡ Russell Vang, MD,*‡ and Deyin Xing, MD, PhD*†‡*

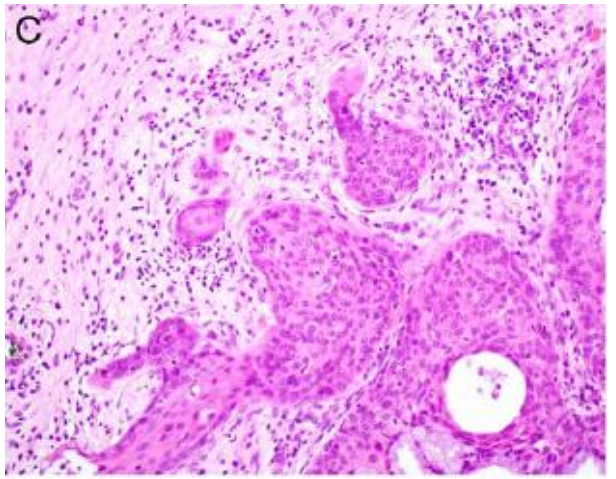

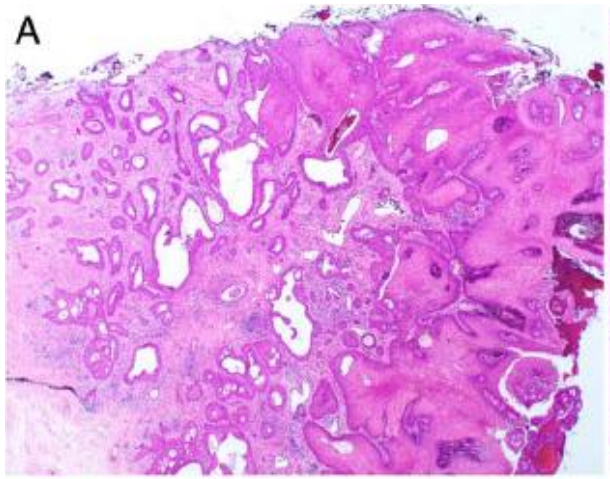

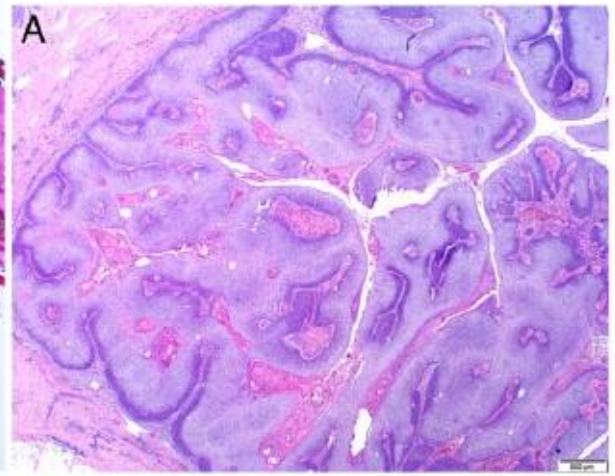

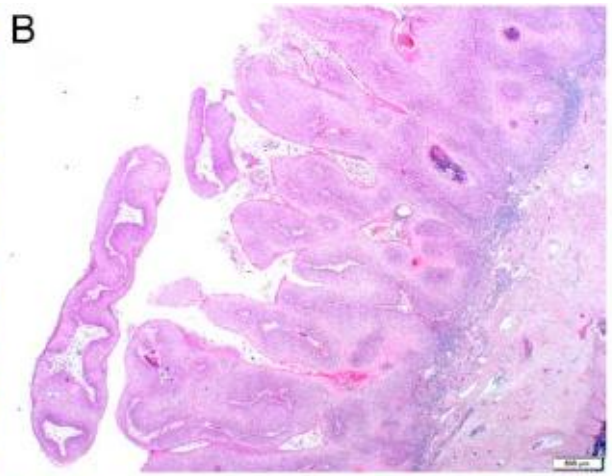

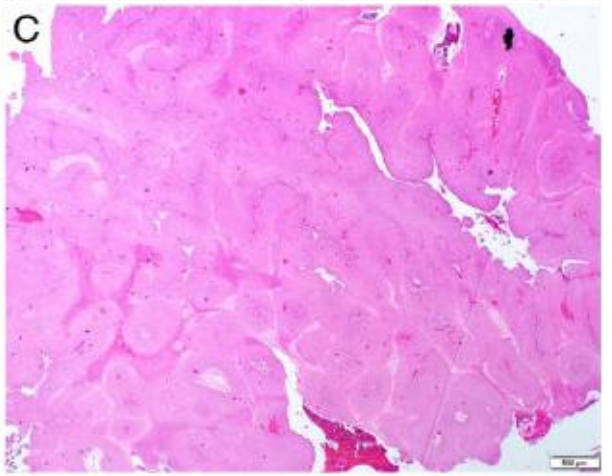

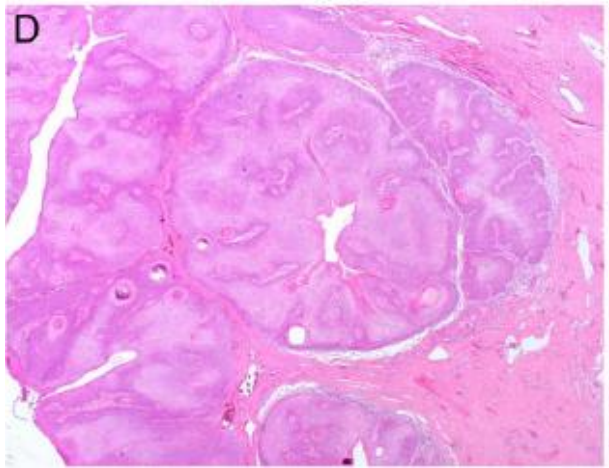

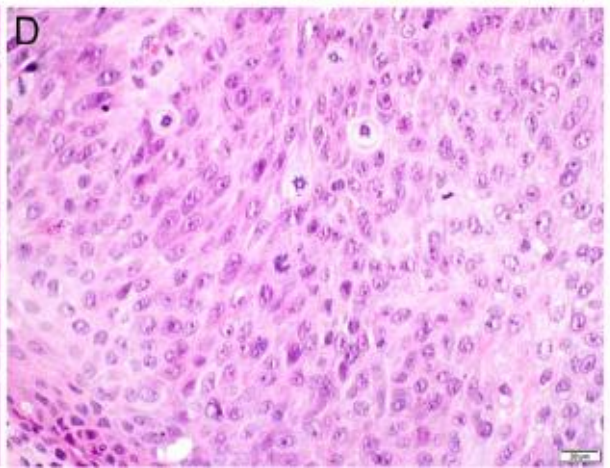

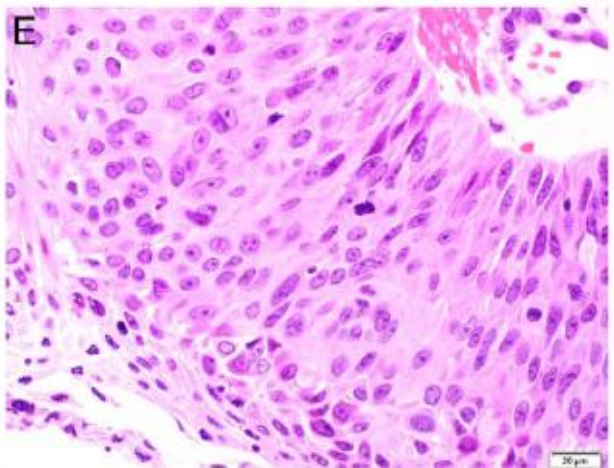

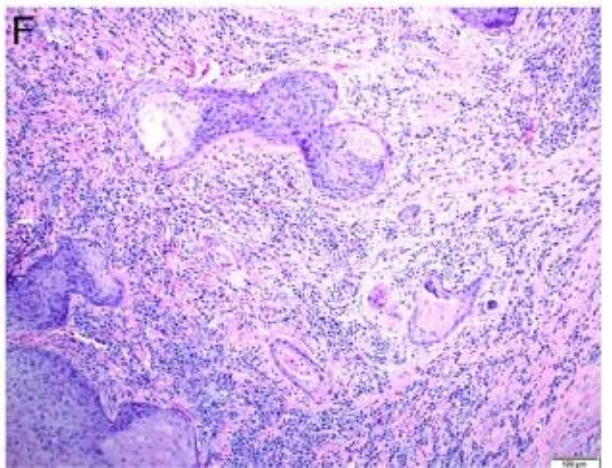

TABLE 2. Gross Findings, Histopathology, HPV, and Immunohistochemistry

Case	Gross findings	Primary lesion location and size	Histology	Depth of invasion	HPV6/11 (RNA ISH)	HPV non-6/11 (RNA ISH)	HPV (PCR)	P16	Ki-67
1	Tan-pink, ectocervical lobulated circumferential nodule, extends to endocervical canal, abutting LUS	Cervix: 3.5 cm	Undulating verruco-papillary lesion with high-grade cytology involving endocervical glands and extending to LUS; stromal invasion; lymphovascular space invasion	0.9 cm	Detected	HR-HPV, HPV16, and HPV18: not detected	HPV6	Focally positive (non-block pattern)	70%-80%
2	Large ectocervical circumferential papillary mass, extends into endocervical canal and focally extends into LUS	Cervix: 4.5 cm	Florid undulating verruco-papillary proliferation with low-grade/bland cytology and extensive endocervical gland involvement; foci suspicious for stromal invasion; transmural involvement of sigmoid colon; liver metastasis	0.1 cm (suspicious, not fully diagnostic)	Detected	HR-HPV: not detected	HPV6	Negative	20%-30%, basal and parabasal layer
3	Tan-white to red, indurated nodular mass	Vulva: 10.7 cm	Florid undulating exophytic and endophytic verruco-papillary lesion with high-grade cytology; focus on superficial stromal invasion	0.1 cm	Detected	HR-HPV: not detected	HPV6	Negative	60%-70%
4	Hair-bearing skin with exophytic lesion	Vulva: 6.6 cm	Florid undulating exophytic and endophytic verruco-papillary lesion with low-grade/bland cytology and stromal reaction; foci of superficial stromal invasion	0.3 cm	Detected*	HR-HPV, HPV16, HPV18: not detected*	HPV6	Focally positive (non-block pattern)	20%-30% basal and parabasal layer
5	White pink markedly rough cervical mucosa	Cervix: fragmented, largest 2 cm	Florid undulating exophytic verruco-papillary lesion with high-grade cytology; 2 foci superficial stromal invasion	0.1 cm	Detected	HR-HPV: not detected	HPV6	Negative	70%-80%
6	Pink-tan to white exophytic tumor extends into LUS	Cervix: 4.7 cm	Florid undulating exophytic verruco-papillary with high-grade cytology and extensive endocervical gland involvement, extending to the vulva, vagina, and urethra	Not identified	Detected	HR-HPV, HPV16, HPV18 and HPV33: not detected	HPV6	Negative	70%-80%
7	Fragments of biopsy tissue	Cervix: biopsy, size not available	Exophytic verruco-papillary lesion with high-grade cytology with stromal invasion; lung and lymph node metastasis	At least 0.4 cm in biopsy specimen	Detected	HR-HPV, HPV16, HPV18 and HPV33: not detected	HPV6	Positive (block pattern)	60%-70%
8	Tan exophytic cauliflower-like nodularity involving entire cervix, extends into LUS and endometrium	Entire cervix (all 18 sections have lesion; size not available)	Undulating verruco-papillary with high-grade cytology replacing entire cervix, extending to vagina and endometrium; multifocal superficial stromal invasion	0.2 cm	Detected	HR-HPV: not detected	HPV11	Negative	70%-80%

HPV-associated endocervical adenocarcinoma

- Binary Silva classification

Int J Gynecol Pathol 2024;43:436–446
Am J Surg Pathol 2024;48:1522–1529

- Utility of Rb immunohistochemistry

Histopathology 2024;84:1178–1191
Mod Pathol 2025;38:100660

Improved Risk Prediction in Human Papillomavirus–Associated Endocervical Adenocarcinoma Through Assessment of Binary Silva Pattern-based Classification: An International Multicenter Retrospective Observational Study Led by the International Society of Gynecological Pathologists (ISGyP)

Aime Powell, PhD, Anjelica Hodgson, MD,†‡ Paul A. Cohen, MD,*§‖*
*Joseph T. Rabban, MD, MPH,¶ Kay J. Park, MD,# W. Glenn McCluggage, FRCPath,***
C. Blake Gilks, MD,††
Contributors from the International Society of Gynecological Pathologists (ISGyP) Endocervical Adenocarcinoma Project‡‡, Naveena Singh, MD,†† and Esther Oliva, MD§§

TABLE 5. Multivariate (adjusted) Competing Risk Model Investigating Factors (Including the 3-tier Silva Pattern of Invasion) Associated With Disease Recurrence and DSS for the Cohort (n = 792)

	Adjusted model					
	Disease recurrence			DSS		
Characteristic	**sHR**	**95% CI**	***P***	**sHR**	**95% CI**	***P***
Age (yr)						
< 50	0.75	0.57–0.98	0.038	0.82	0.35–2.05	0.719
≥ 50	1.0	—	—	1.0	—	—
FIGO stage						
Stage IA2	0.34	0.11–0.99	0.048	0.56	0.10–3.15	0.672
Stage IB1	1.0	—	—	1.0	—	—
Stage IB2	1.08	0.74–1.58	0.683	1.29	0.65–2.59	0.470
Stage IB3	0.73	0.22–2.42	0.605	0.95	0.12–7.43	0.965
Lymphovascular invasion status						
Absent	1.0	—	—	1.0	—	—
Present	1.83	1.24–2.72	0.003	3.91	1.52–10.08	0.005
Silva pattern of invasion						
Pattern A	0.36	0.16–0.82	0.016	0.32	0.13–0.79	0.013
Pattern B	0.55	0.31–0.98	0.042	0.65	0.16–2.57	0.540
Pattern C	1.0	—	—	1.0	—	—

DSS, disease-specific survival; FIGO, International Federation of Gynecology and Obstetrics; sHR, subdistribution hazard ratio.

TABLE 7. Multivariate (adjusted) Competing Risk Model Investigating Factors (Including the Silva Pattern of Invasion as a Binary Classification System) Associated With Disease Recurrence and DSS for the Cohort (n = 792)

	Adjusted model					
	Disease recurrence			DSS		
Characteristic	**sHR**	**95% CI**	***P***	**sHR**	**95% CI**	***P***
Age (yr)						
< 50	0.70	0.52–0.94	0.017	0.82	0.35–1.94	0.657
≥ 50	1.0	—	—	1.0	—	—
FIGO stage						
Stage IA2	0.33	0.10–1.02	0.055	0.58	0.11–3.01	0.513
Stage IB1	1.0	—	—	1.0	—	—
Stage IB2	1.17	0.79–1.73	0.423	1.43	0.70–2.92	0.332
Stage IB3	0.84	0.25–2.80	0.780	1.31	0.16–10.95	0.801
Silva pattern of invasion						
Pattern A and pattern B (−LVSI)	0.40	0.24–0.65	0.000	0.25	0.08–0.77	0.016
Pattern B (+LVSI) and pattern C	1.0	—	—	1.0	—	—

DSS, disease-specific survival; FIGO, International Federation of Gynecology and Obstetrics; LVSI, lymphovascular space invasion; sHR, subdistribution hazard ratio.

TABLE 2. Characteristics of the Study Cohort (n = 792), Stratified by Silva Pattern of Invasion

Characteristic	Silva pattern of invasion: Pattern A (n = 198); n (%)	Pattern B (no LVSI; n = 195); n (%)	Pattern B (+ LVSI; n = 65); n (%)	Pattern C (n = 334); n (%)	*P*
Age (yr)					
< 50	149 (75.3)	151 (77.4)	56 (86.2)	226 (67.7)	0.005
≥ 50	49 (24.7)	44 (22.6)	9 (13.8)	108 (32.3)	—
FIGO stage					
IA2	49 (24.8)	34 (17.4)	7 (10.8)	22 (6.6)	—
IB1	107 (54.0)	106 (54.4)	32 (49.2)	153 (45.8)	0.000
IB2	36 (18.2)	48 (24.6)	22 (33.9)	127 (38.0)	—
IB3	6 (3.0)	7 (3.6)	4 (6.1)	32 (9.6)	—
IECC/WHO tumor type					
HPV adenocarcinoma, usual type	189 (95.4)	188 (96.4)	58 (89.2)	307 (91.2)	0.053
HPV adenocarcinoma, mucinous intestinal type	9 (4.6)	5 (2.6)	5 (7.7)	21 (6.3)	—
HPV adenocarcinoma, mucinous NOS type	—	2 (1.0)	2 (3.1)	2 (0.6)	—
HPV adenocarcinoma, mucinous signet-ring cell type	—	—	—	4 (1.2)	—
Tumor grade					
G1	153 (77.3)	87 (44.6)	19 (29.2)	68 (20.4)	0.000
G2	43 (21.7)	94 (48.2)	41 (63.1)	222 (66.5)	—
G3	1 (0.5)	4 (2.1)	3 (4.6)	37 (11.0)	—
Not reported	1 (0.5)	10 (5.1)	2 (3.1)	7 (2.1)	—
Lymphovascular invasion status					
Absent	198 (100)	195 (100)	—	215 (64.4)	0.000
Present	—	—	65 (100)	119 (35.6)	—
Most extensive surgery performed					
Excisional biopsy (CKC or LEEP)	2 (1.0)	2 (1.0)	—	2 (0.6)	0.016
Trachelectomy	15 (7.6)	20 (10.3)	8 (12.3)	20 (6.0)	—
Extrafascial hysterectomy (± BSO)	20 (10.1)	15 (7.7)	—	14 (4.2)	—
Radical hysterectomy (± BSO)	161 (81.3)	158 (81.0)	57 (87.7)	298 (89.2)	—
Recurrence					
Yes	7 (3.5)	12 (6.2)	6 (9.2)	48 (14.4)	0.000
No	191 (96.5)	183 (93.8)	59 (90.8)	286 (85.6)	—
Outcome					
Alive	194 (98.0)	192 (98.5)	62 (95.4)	321 (96.1)	0.041
Died of disease	1 (0.5)	2 (1.0)	3 (4.6)	12 (3.6)	—
Died of unrelated causes*	3 (1.5)	1 (0.5)	—	1 (0.3)	—

BACK

Assessment of Interobserver Agreement Among Gynecologic Pathologists Between Three-Tier Versus Binary Pattern-based Classification Systems for HPV-associated Endocervical Adenocarcinoma

Roman E. Zyla, MD,† David W. Dodington, MD MSc,*† Sara Pakbaz, MD,*‡ Tatjana Terzic, MD,*‡ Carrie Robinson, MD,*‡ Blaise Clarke, MD,*† Marjan Rouzbahman, MD,*† and Anjelica Hodgson, MD*†*

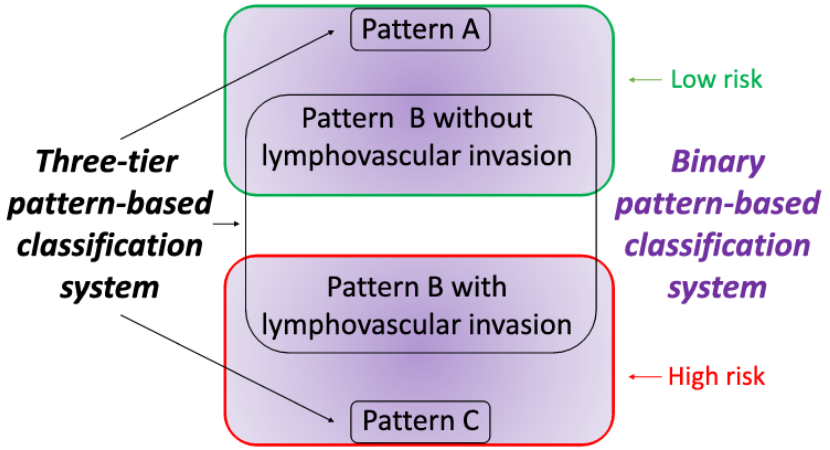

3/5 reviewers showed no intraobserver discrepancy while the remaining 2 did in a small subset of cases (n = 2 and 4, respectively).

TABLE 1. Overall Interobserver Results with Assignment for Three-tier and Binary Pattern-based Classification Systems of HPV-associated Endocervical Adenocarcinoma

	2-3/5 reviewers in agreement, n (%)	4/5 reviewers in agreement, n (%)	5/5 reviewers in agreement, n (%)	Kappa	SE	95% Confidence Interval	*P*
A vs. B vs. C	16 (27)	15 (25)	28 (48)	0.564 (moderate)	0.030	0.562-0.566	< 0.001
Low risk vs. high risk	8 (14)	14 (24)	37 (62)	0.634 (good/ substantial)	0.041	0.631-0.636	< 0.001
LVI	11 (19)	12 (20)	36 (61)	0.560 (moderate)	0.041	0.557-0.562	< 0.001

LVI indicates lymphovascular invasion; SE, standard error; *P*, p value.

Immunohistochemical p16 overexpression and Rb loss correlate with high-risk human papillomavirus infection in endocervical adenocarcinomas

Nobuko Yasutake,[1,2] Hidetaka Yamamoto,[3,4] Ryosuke Kuga,[4,5] Rina Jiromaru,[5] Takahiro Hongo,[5] Yoshihiro Katayama,[1,4] Kenzo Sonoda,[6] Hideaki Yahata,[1] Kiyoko Kato[1] & Yoshinao Oda[4]

[1]*Department of Gynecology and Obstetrics, Graduate School of Medical Sciences, Kyushu University, Fukuoka,* [2]*Department of Gynecology and Obstetrics, Japan Community Healthcare Organization Kyushu Hospital, Kitakyushu,* [3]*Department of Pathology, Graduate School of Medicine, Dentistry and Pharmaceutical Science, Okayama University, Okayama,* [4]*Department of Anatomic Pathology, Pathological Sciences, Graduate School of Medical Sciences,* [5]*Department of Otorhinolaryngology, Graduate School of Medical Sciences, Kyushu University and* [6]*Department of Gynecology and Obstetrics, National Kyushu Cancer Center, Fukuoka, Japan*

Table 2. The reliability of immunohistochemical expression pattern of p16 and Rb to predict HR-HPV infection

	Sensitivity	Specificity	PPV	NPV
ECAs (n = 108)				
p16^{+} alone	100	84	95.4	100
p16+/Rb partial loss	100	100	100	100
ECAs and adenocarcinoma of endometrium or equivocal origin (n = 121)				
p16^{+} alone	100	73.6	89.2	100
p16+/Rb partial loss	100	100	100	100

ECA, endocervical adenocarcinoma; HR, high-risk; HPV, human papillomavirus; NPV, negative predictive value; PPV, positive predictive value.

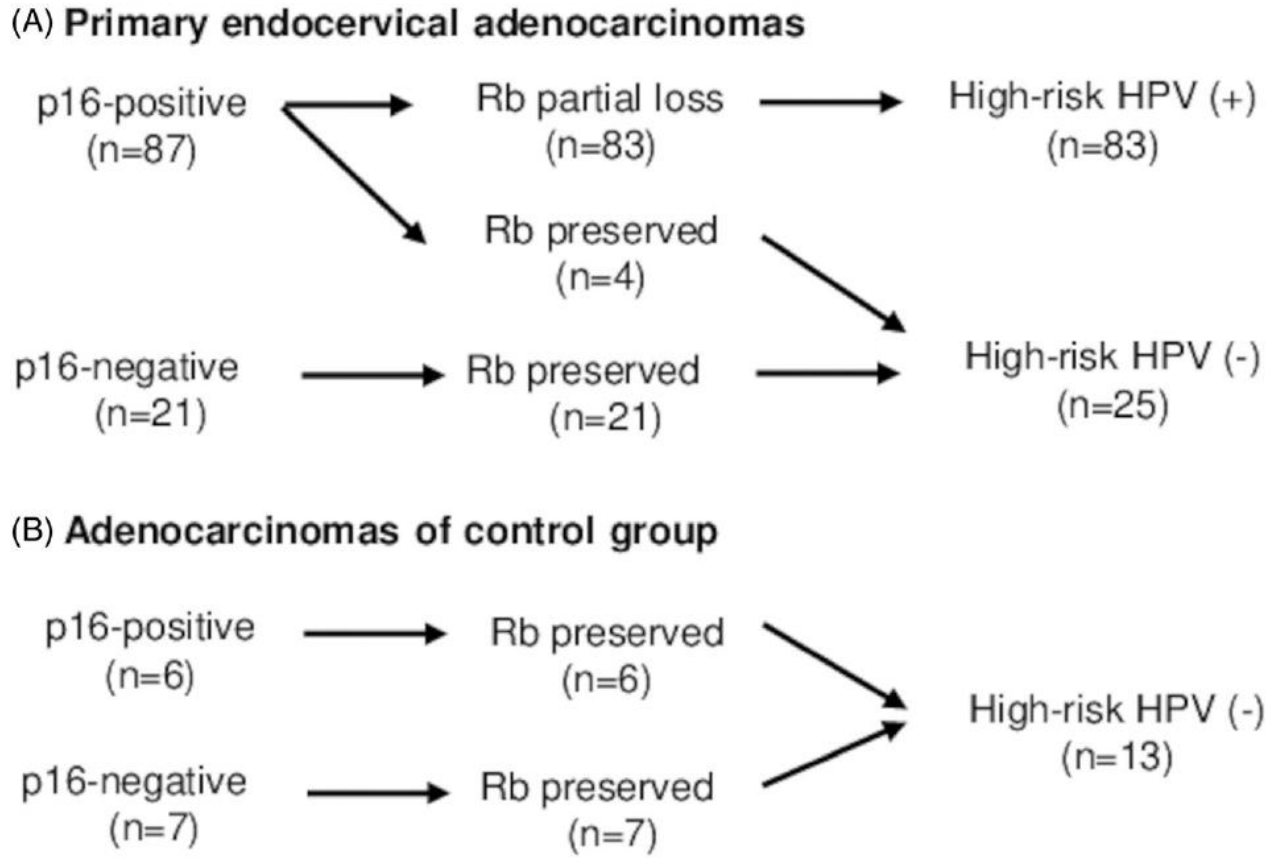

Retinoblastoma Protein Loss in p53 Abnormal Endometrial Carcinoma: Histologic and Clinicopathological Correlates

Ezgi Dicle Serbes[a], Nanda Horeweg[b], Carlos Parra-Herran[c], Renske van Rijnsoever[d], Jan J. Jobsen[e], Ina Jurgenliemk-Schulz[f], Nienke Kuijsters[g], Remi A. Nout[b], Marie A.D. Haverkort[h], Melanie E. Powell[i], Pearly Khaw[j], Marie Plante[k], Catherine Genestie[l], Hans W. Nijman[m], Carien L. Creutzberg[b], Tjalling Bosse[d,*], Claire J.H. Kramer[d]

16 / 227 (7%) p53-abnormal endometrial carcinomas

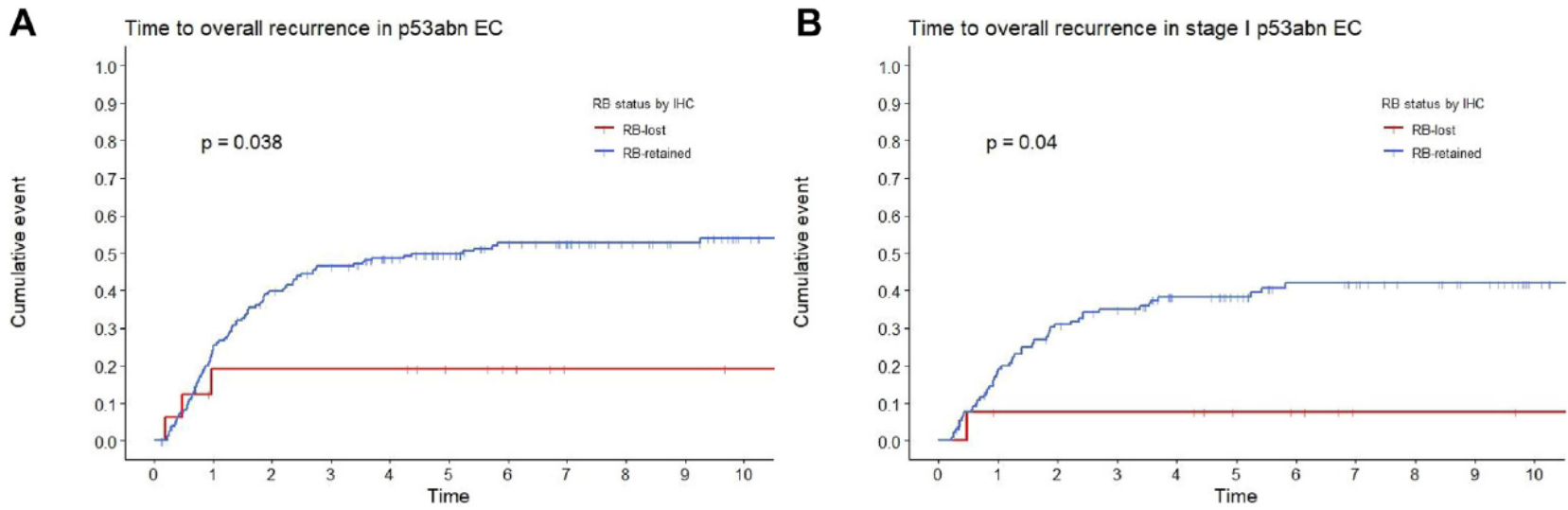

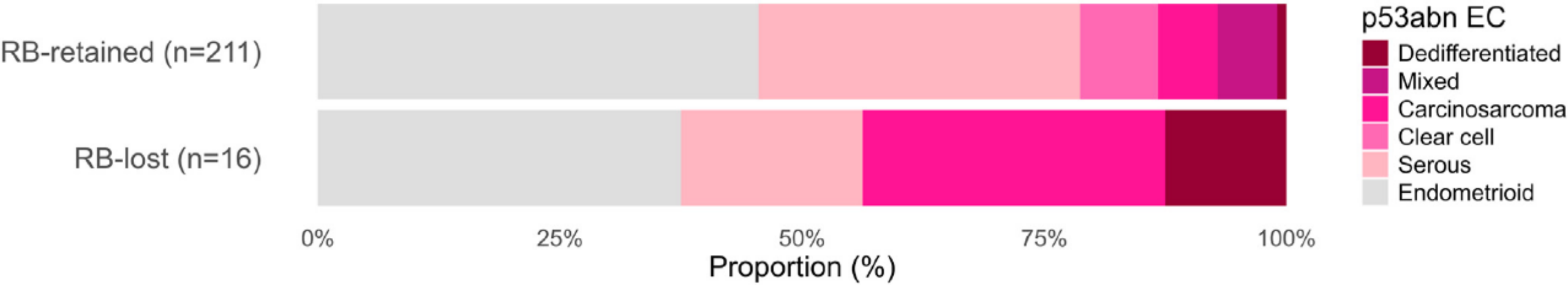

Gastric-type adenocarcinoma

- Utility of Claudin 18 immunohistochemistry

Mod Pathol 2024;37:100569
Am J Surg Pathol 2025;49:206–216

- Endometrial gastric-type adenocarcinoma

Am J Surg Pathol 2025;49:564–577

The Clinicopathological and Molecular Characteristics of Endocervical Gastric-Type Adenocarcinoma and the Use of Claudin18.2 as a Potential Therapeutic Target

Jing Yang[a], Yang Peng[b], Yan Ding[c], Yueping Liu[c], Yuxiang Wang[a], Yan Liu[a], Congrong Liu[a,*]

[a] *Department of Pathology, Third Hospital, School of Basic Medical Sciences, Peking University Health Science Center, Beijing, China;* [b] *Fourth Department of Gyneco... Hunan Cancer Hospital/The Affiliated Cancer Hospital of Xiangya School of Medicine, Central South University, Changsha, China;* [c] *Department of Pathology, The Fou... Hebei Medical University, Shijiazhuang, Hebei, China*

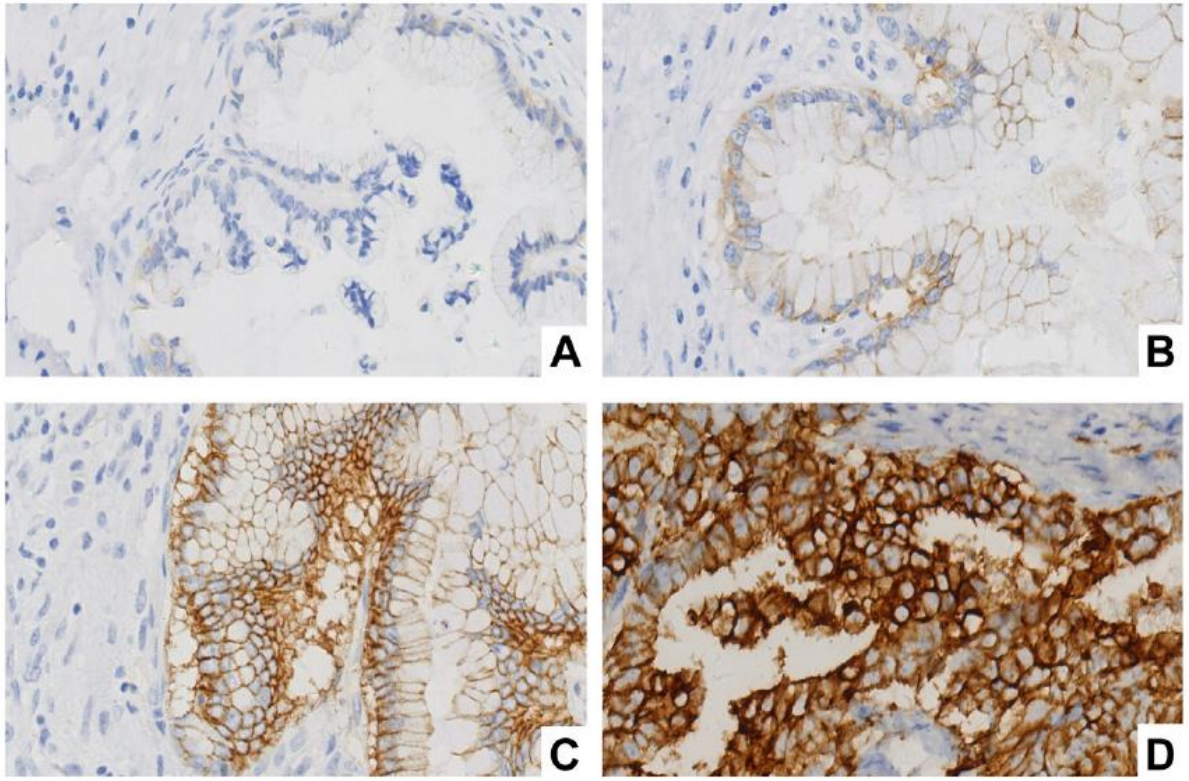

Table 2

Immunohistochemistry of gastric markers in GAS and other diseases

Markers	GAS % (n = 62)	HPVA % (n = 34)		Endometrioid carcinoma with mucinous differentiation % (n = 22)	Endocervical metastatic mucinous adenocarcinoma % (n = 14)	Normal cervicalmucosa % (n = 22)
		Usual type % (n = 24)	Mucinous type % (n = 10)			
Claudin 18.2	95.2 (59/62)	0 (0/24)	10 (1/10)	0 (0/22)	7.1 (1/14)	0 (0/22)
Muc6	89 (55/62)	66.7 (16/24)	100 (10/10)	50 (11/22)	57.1 (8/14)	63.6 (14/22)
Hik1083	67.7 (42/62)	0 (0/24)	20 (2/10)	0 (0/22)	14.3 (2/14)	0 (0/22)

GAS, endocervical gastric-type adenocarcinoma; HPVA, HPV-associated endocervical adenocarcinoma.

BACK

Claudin-18 and Mutation Surrogate Immunohistochemistry in Gastric-type Endocervical Lesions and their Differential Diagnoses

Lawrence Hsu Lin, MD, PhD,† Harsimar Kaur, MBBS,* David L. Kolin, MD, PhD,* Marisa R. Nucci, MD,* and Carlos Parra-Herran, MD**

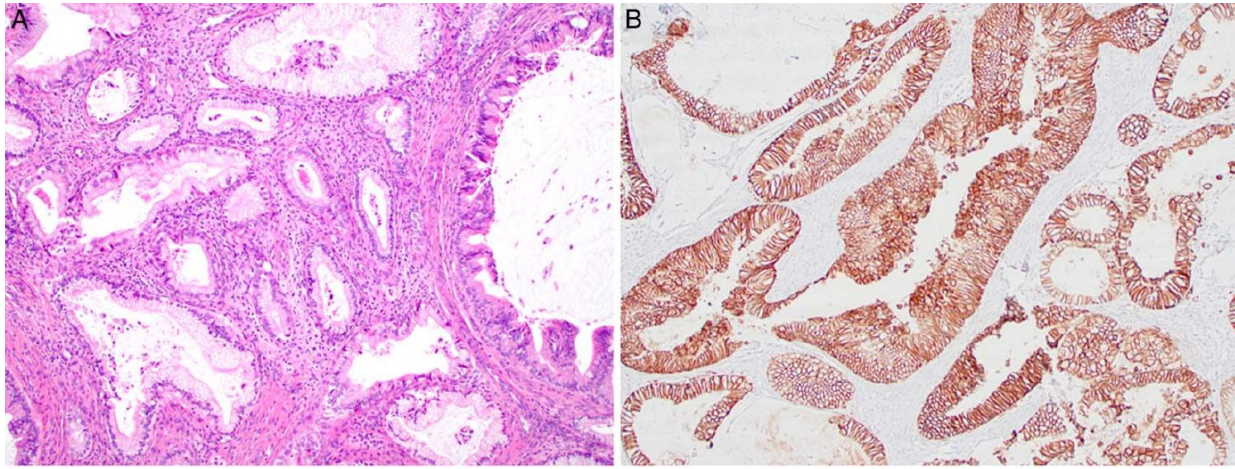

TABLE 1. Immunohistochemical Expression of claudin-18, Progesterone Receptor (PR), P53, STK11/LKB1, MTAP, and SMAD4 in gastric-type Endocervical Adenocarcinoma (GAS) in Comparison to Benign gastric-type Lesions, Including Lobular Endocervical Glandular Hyperplasia (LEGH), and Benign Mullerian Endocervical Specimens

	Gastric-type endocervical adenocarcinoma (n = 46)	Benign gastric-type lesions and LEGH (n = 12)	Benign Mullerian endocervical gland populations (n = 54)	*P*
Claudin-18, n (%)				
Positive	36 (78)	12 (100)	0	< 0.0001*
Negative	10 (22)	0	54 (100)	
Progesterone receptor (PR), n (%)				
Positive	0	0	11 (92)	< 0.0001*
Negative	22 (100)	5 (100)	1 (8)	
P53, n (%)				0.0019*
Normal	28 (65)	10 (100)	15 (100)	
Abnorma	15 (35)	0	0	
STK11/LKB1, n (%)				
Normal	33 (75)	8 (73)	25 (100)	0.0078*
Abnormal	11 (25)	3 (27)	0	
MTAP, n (%)				
Normal	27 (77)	10 (100)	14 (100)	0.049*
Abnormal	8 (23)	0	0	
SMAD4/DPC4, n (%)			0.99	
Normal	21 (91)	4 (100)	6 (100)	
Abnormal	2 (9)	0	0	

Primary Endometrial Gastric (Gastrointestinal)-type Mucinous Adenocarcinoma

A Detailed Clinicopathologic and Molecular Analysis of 27 Cases

Harsimar Kaur, MBBS,† Lawrence Hsu Lin, MD, PhD,*‡ David L. Kolin, MD, PhD,* Andre Pinto, MD,§ Carlos Parra-Herran, MD,* Mark Catherwood, MD,‖ Koen Van de Vijver, MD, PhD,¶ Natalia Buza, MD,† W. Glenn McCluggage, FRCPath,# and Marisa R. Nucci, MD**

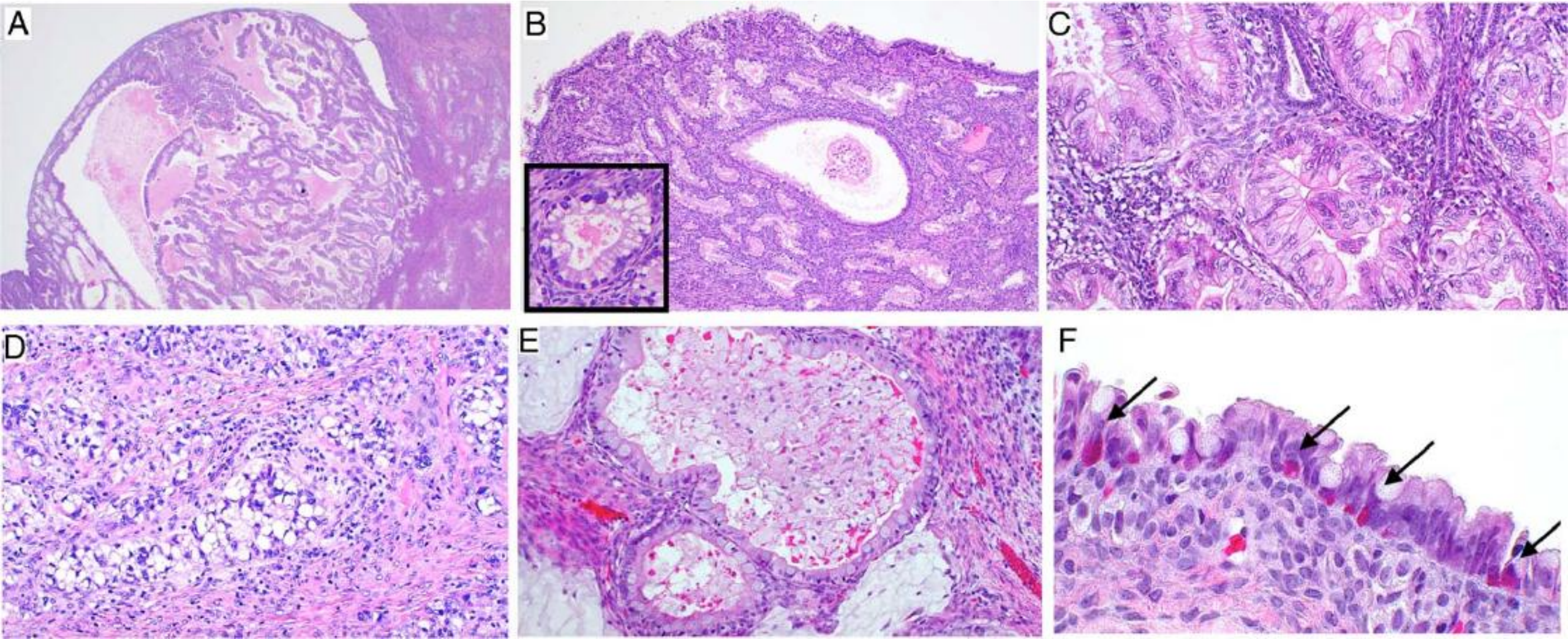

Case ID	%	1	2	4	5	6	7	9	10	11	12	14	15	17	18	19	21	23	25	26	27
TMB		6.1	ND	12.9	35	ND	ND	ND	ND	ND	4.6	ND	19	ND	ND	4.6	13.7	ND	4.6	ND	ND
TP53	65								*					*				*	*		
KRAS	35																				
PIK3CA	25																				
BRCA2	20																				
SMAD4	15																				
FBXW7	15																				
ARID1A	10																				
CDKN2A	10																				
MMR	10																				
ATM	10																				
ERBB2	10																				
CCNE1	10																				
MYC	10																				
STK11	10																				
PPP2R1A	5																				
POLE	5																				
PTEN	5																				
BRAF	5																				

TMB- Total mutation burden (mut/Mb),
ND- Not done,
*p53 wild-type by IHC

Missense Mutation
Nonsense Mutation
Frameshift Mutation
Amplification
Single copy deletion
Double copy deletion
Microsatellite instability-high
MLH1 hypermethylated
MLH1 not methylated

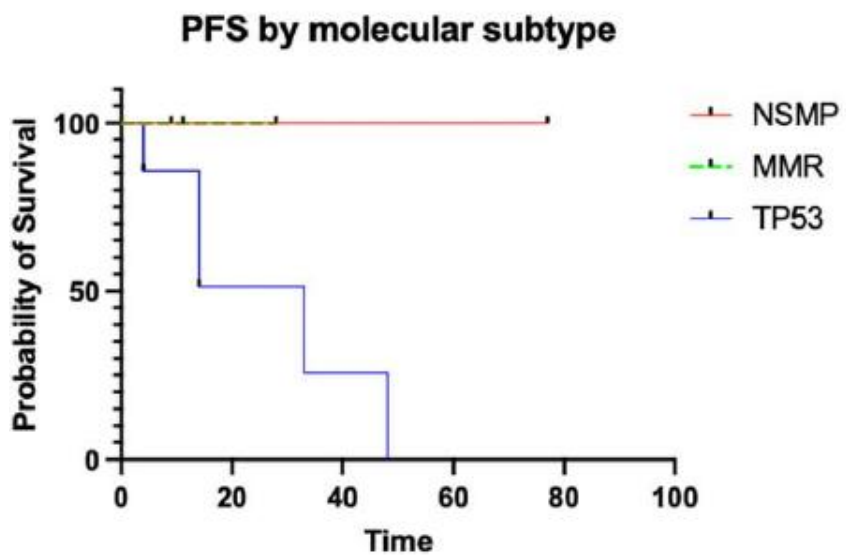

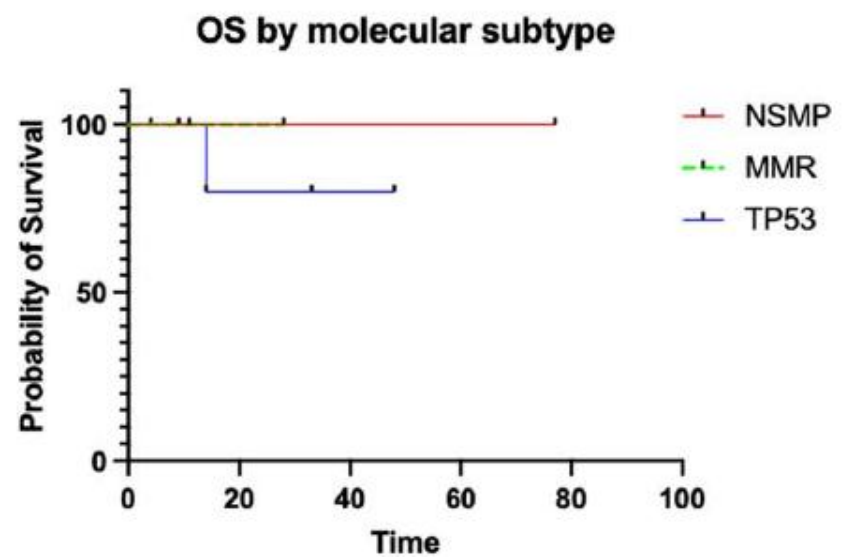

Endometrial carcinoma

- Experience with implementation of molecular classification

Histopathology 2025;86:611–626
Int J Gynecol Pathol 2024;43:335–348

- ER expression in high grade NSMP endometrial cancers

Histopathology 2024;85:660–670
Int J Gynecol Pathol 2025 PMID 40433960

Initiation of molecular testing of endometrial carcinomas in a population-based setting: practical considerations and pitfalls

Jesús Machuca-Aguado,[1] Mark Catherwood,[2] Oisin Houghton,[3] Jennifer Taylor,[3] Rajeev Shah,[4] Ali Ben-Mussa,[5] David Gonzalez[6] & W Glenn McCluggage[3]

[1]Department of Pathology, Virgen Macarena University Hospital, Seville, Spain, [2]Regional Molecular Diagnostics Service, [3]Department of Pathology, Belfast Health and Social Care Trust, Belfast, [4]Department of Pathology, Southern Health and Social Care Trust, Craigavon, [5]Department of Pathology, Western Health and Social Care Trust, Londonderry, Northern Ireland and [6]Patrick G Johnston Centre for Cancer Research, Queen's University Belfast, Belfast, UK

Herein we present our experience in initiating molecular testing of all ECs in Northern Ireland, a country with a relatively stable population and an integrated pathology laboratory information system. To the best of our knowledge, this represents one of the first unbiased population-based studies investigating the prevalence of the different TCGA molecular groups of EC.

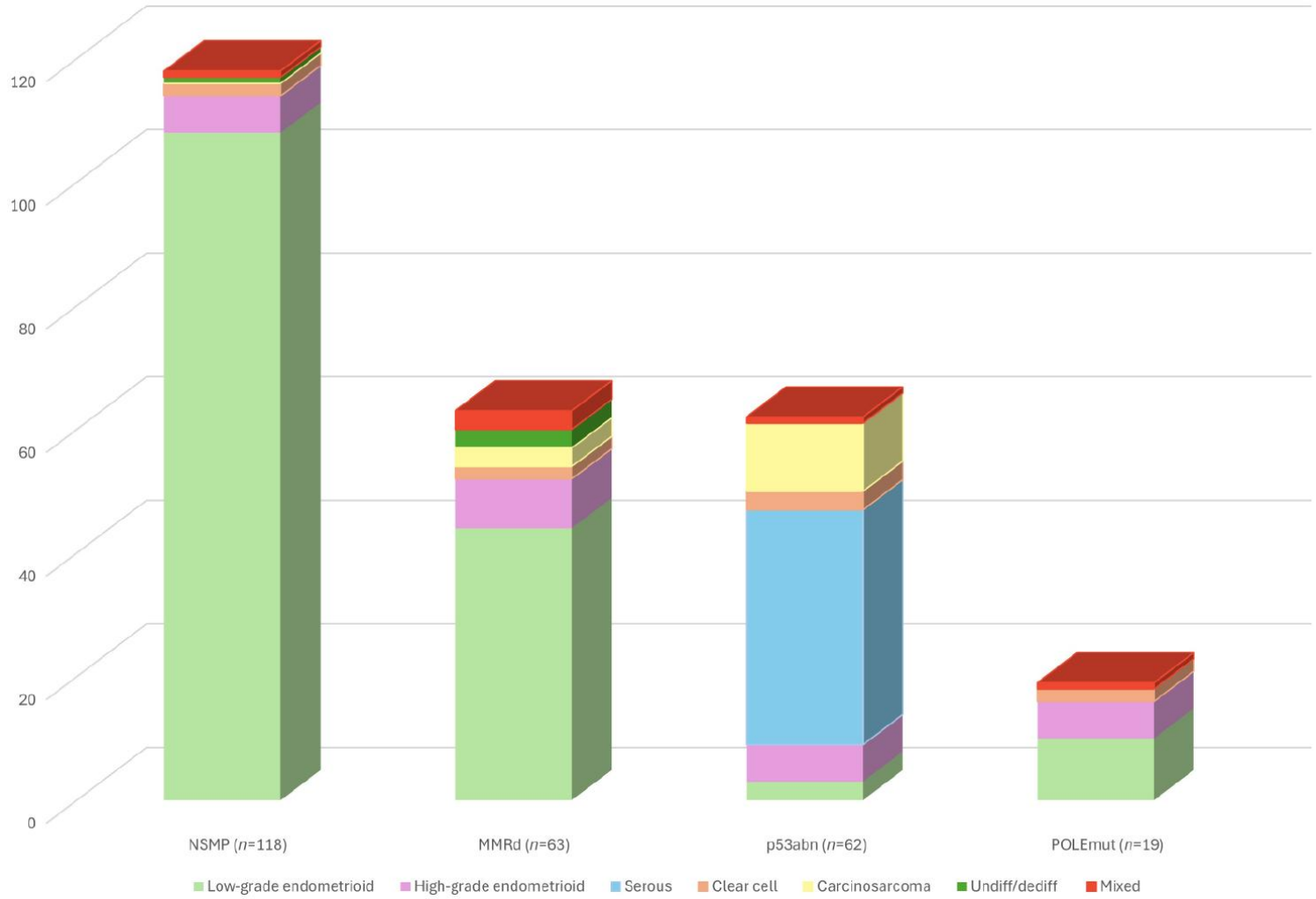

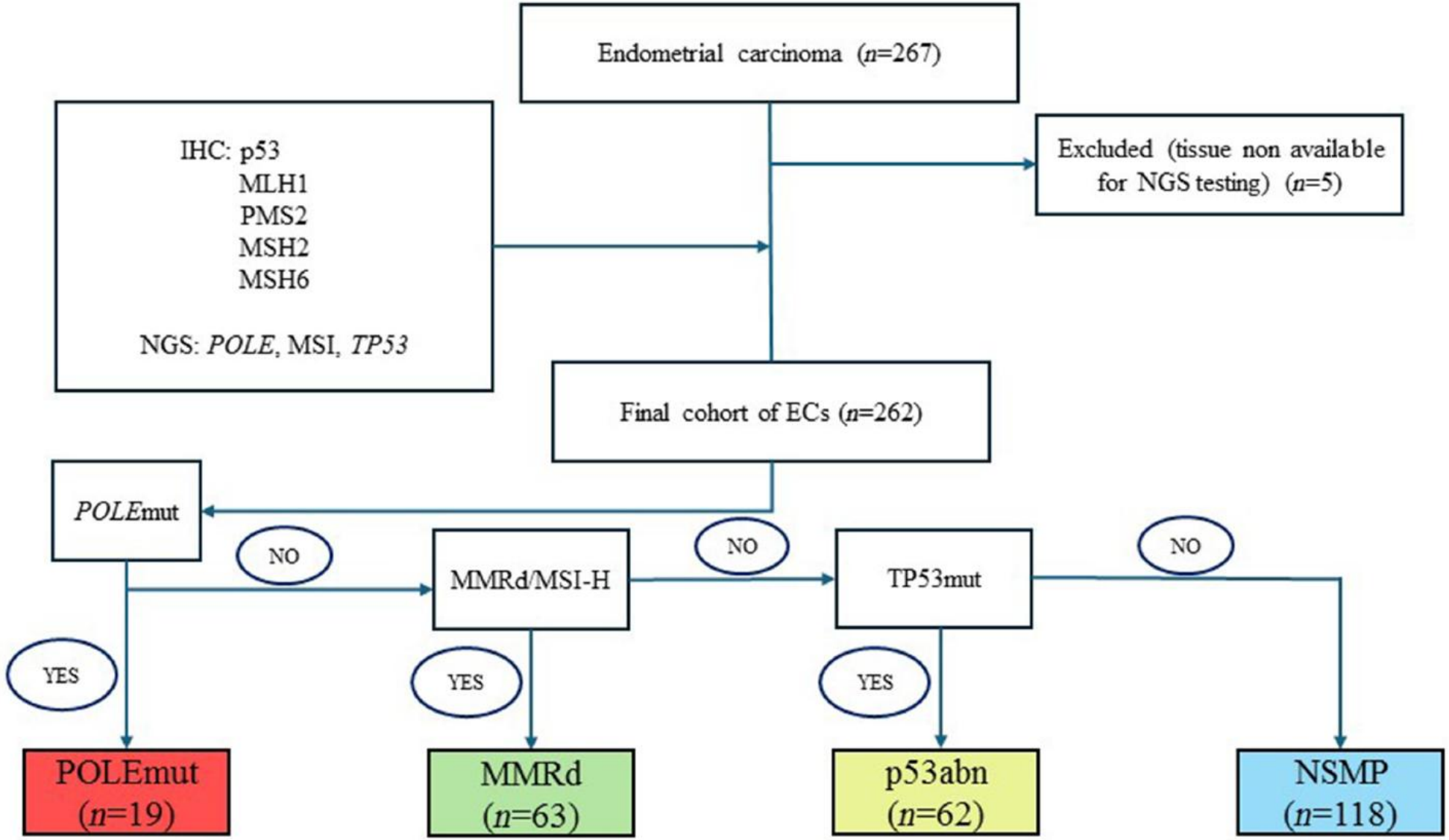

- p.Pro286Arg (c.857C>G) (*n*=8)
- p.Val411Leu (c.1231G>C) (*n*=7)
- p.Ser297Phe (c.890C>T) (*n*=2)
- p.Ala465Val (c.1394C>T) (*n*=1)
- p.Ser461Thr (c.1381T>A) (*n*=1)

- MSH2 and MSH6 loss (*n*=7)
- MSH6 loss (*n*=7)
- MLH1 and PMS2 loss (*n*=43)
- PMS2 loss (*n*=3)
- MMRp/MSI-H (*n*=3)

- Diffuse mutation-type IHC (*n*=43)
- Null mutation-type IHC (*n*=7)
- Subclonal diffuse/null mutation-type IHC (*n*=2)
- Wild type IHC /TP53mut on NGS (*n*=10)

Prospective Clinical Prognostication of Endometrial Carcinomas Based on Next-Generation Sequencing and Immunohistochemistry—Real-World Implementation and Results at a Tertiary Care Center

Kurtis D. Davies, Ph.D., Lynelle P. Smith, M.D., Amy Guimaraes-Young, M.D., Ph.D., Bradley R. Corr, M.D., Christine M. Fisher, M.D., M.P.H., Saketh R. Guntupalli, M.D., Amber A. Berning, M.D., Miriam D. Post, M.D., Devon Pino, M.D., Dara L. Aisner, M.D., Ph.D., and Rebecca J. Wolsky, M.D.

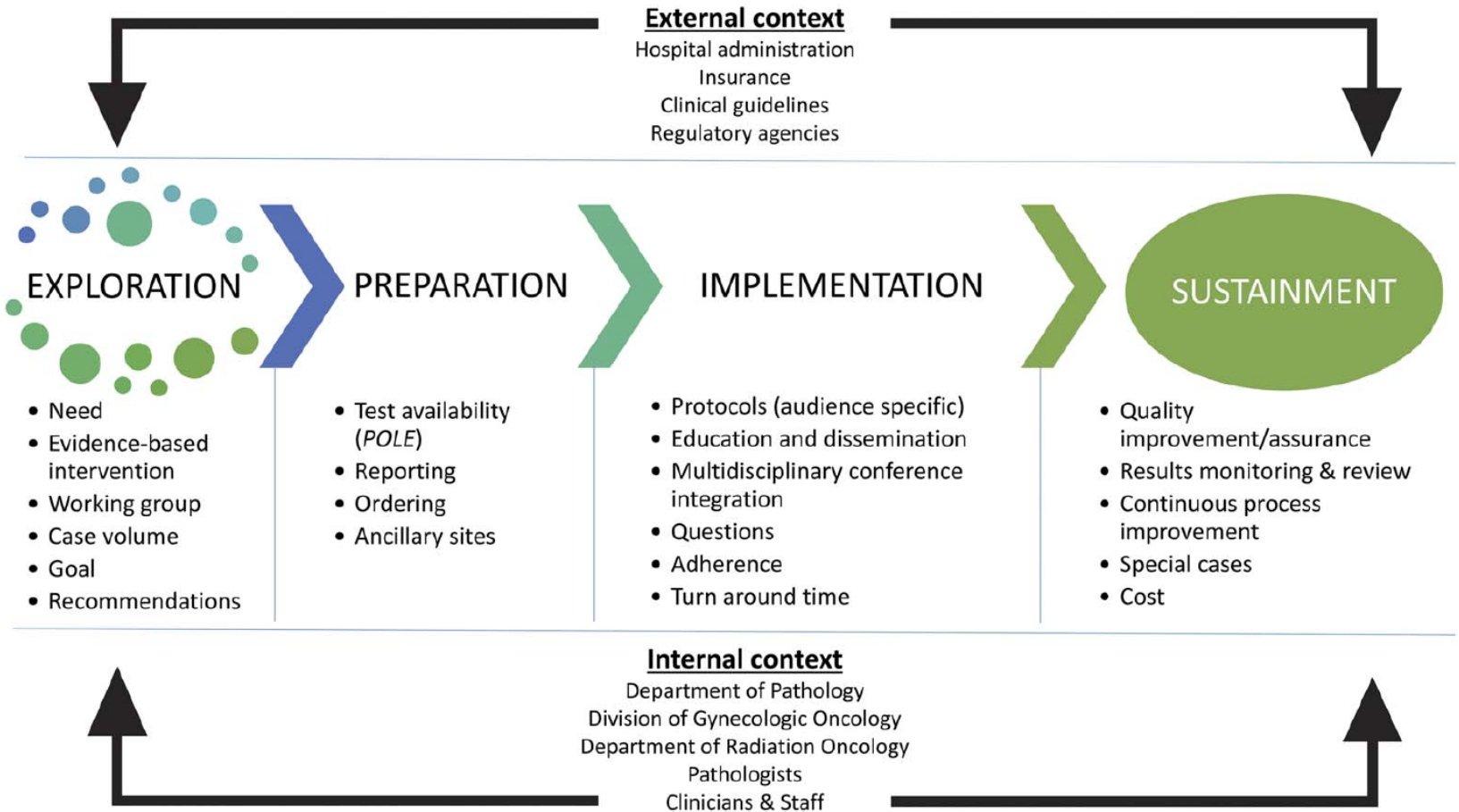

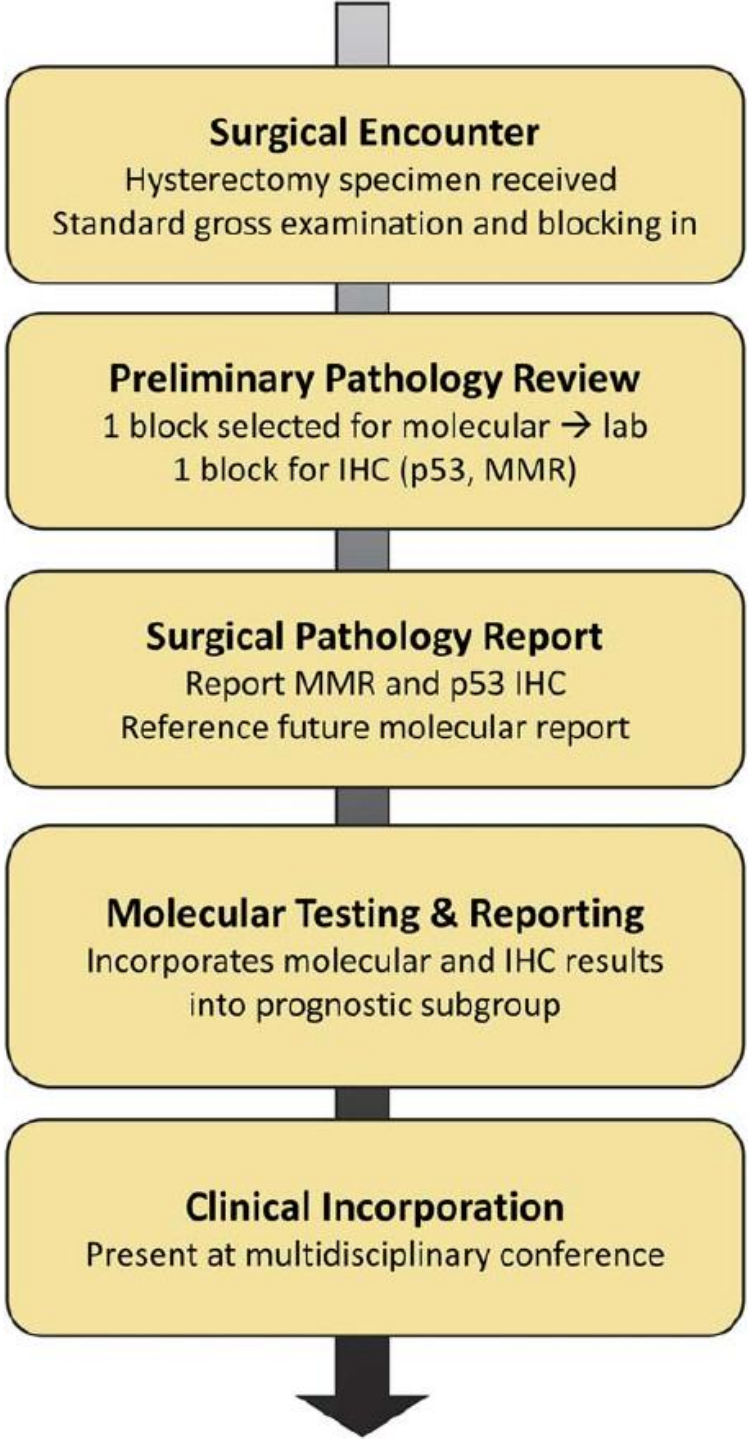

BACK

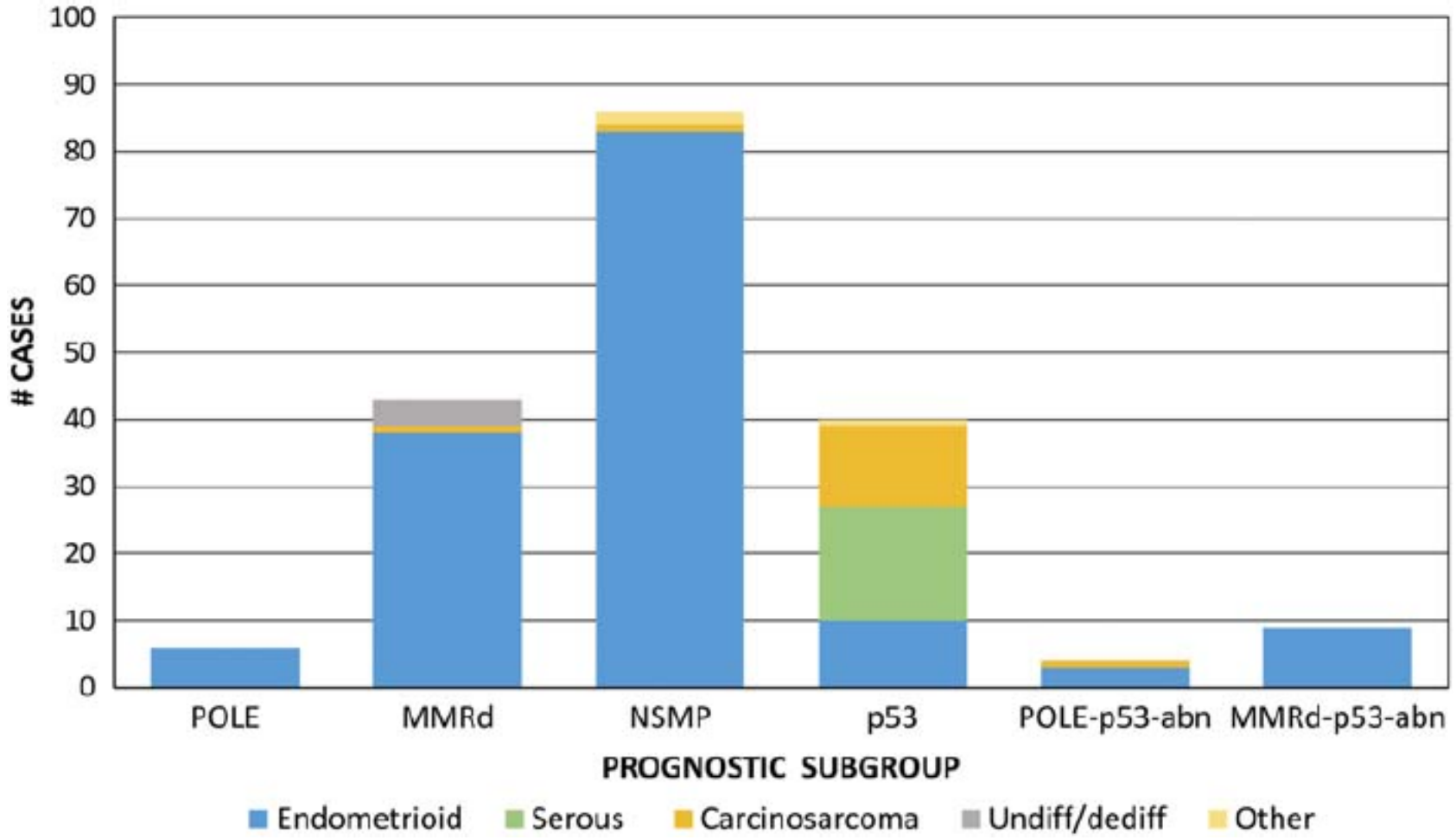

TABLE 4. *Gene or pathway mutational rates (percentage of cases) per prognostic subgroup*

	AKT1	*BRAF*	*CTNNB1*	*FGFR2*	*KRAS*	*PIK3CA*	*PIK3R1*	*PTEN*	*TP53*	PI3K path activated
POLE	0.0	30.0	20.0	20.0	30.0	90.0	20.0	90.0	40.0	100.0
MMRd	3.8	0.0	5.8	21.2	30.8	57.7	36.5	88.5	15.4	96.2
NSMP	9.3	3.5	31.4	12.8	27.9	47.7	44.2	79.1	0.0	95.3
p53-abn	2.5	0.0	5.0	5.0	12.5	37.5	22.5	32.5	100.0	70.0

MMRd indicates mismatch repair deficient; NSMP, no specific molecular profile; p53-abn, p53 abnormal.

The spectrum of oestrogen receptor expression in endometrial carcinomas of no specific molecular profile

Mona Alafraidi,[1,2,3] Lynn Hoang,[2,3] Brooke E. Howitt,[4] Teri A. Longacre,[4] Jessica N. McAlpine,[5] Amy Jamieson,[5] Naveena Singh,[2,3,†] C Blake Gilks[2,3] & Jennifer Pors[1,2]

[1]Department of Pathology, British Columbia Cancer Agency, [2]Department of Pathology and Laboratory Medicine, University of British Columbia, [3]Department of Pathology and Laboratory Medicine, Vancouver General Hospital, Vancouver, BC, Canada, [4]Department of Pathology, Stanford University School of Medicine, Stanford, CA, USA and [5]Division of Gynecologic Oncology, Department of Obstetrics and Gynecology, University of British Columbia, Vancouver, BC, Canada

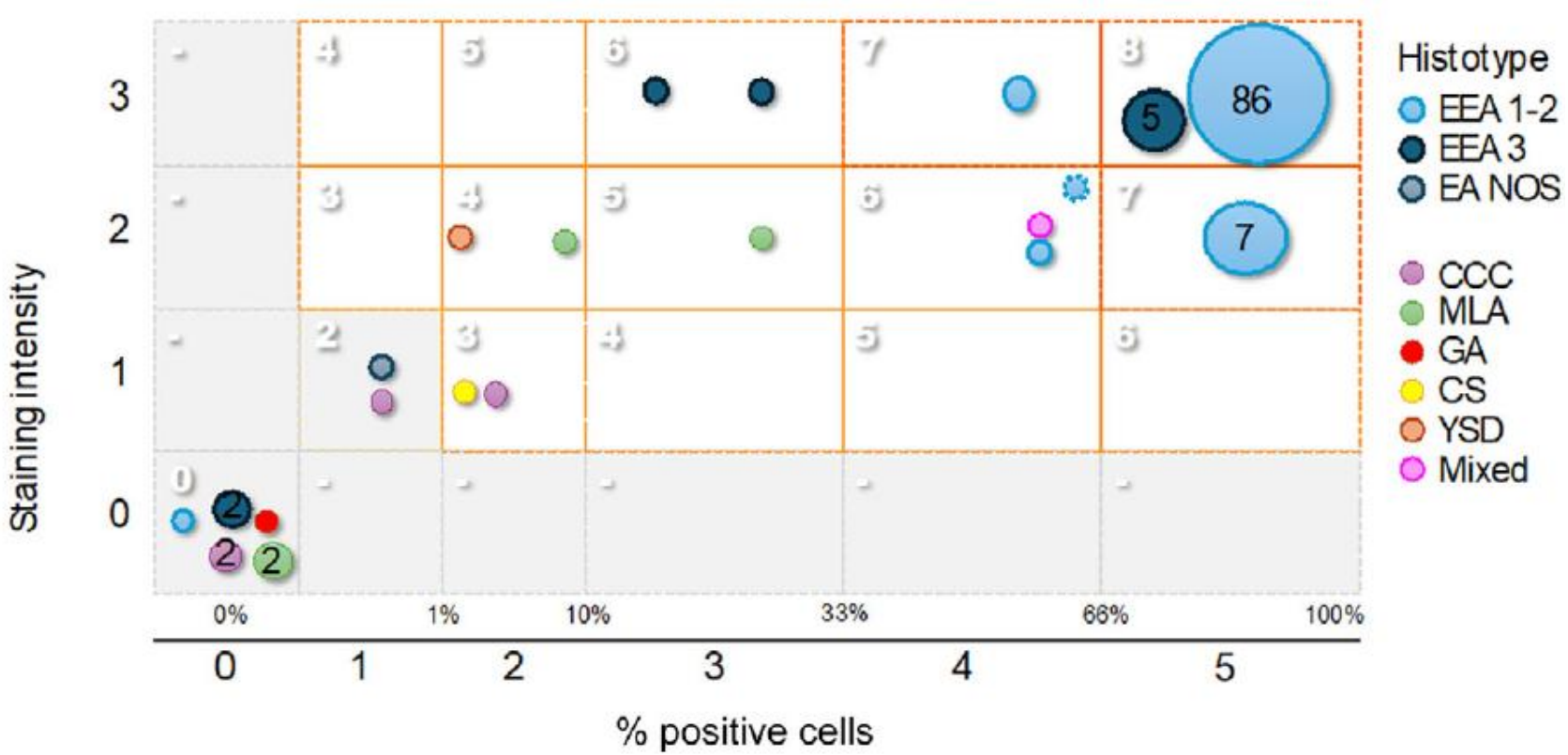

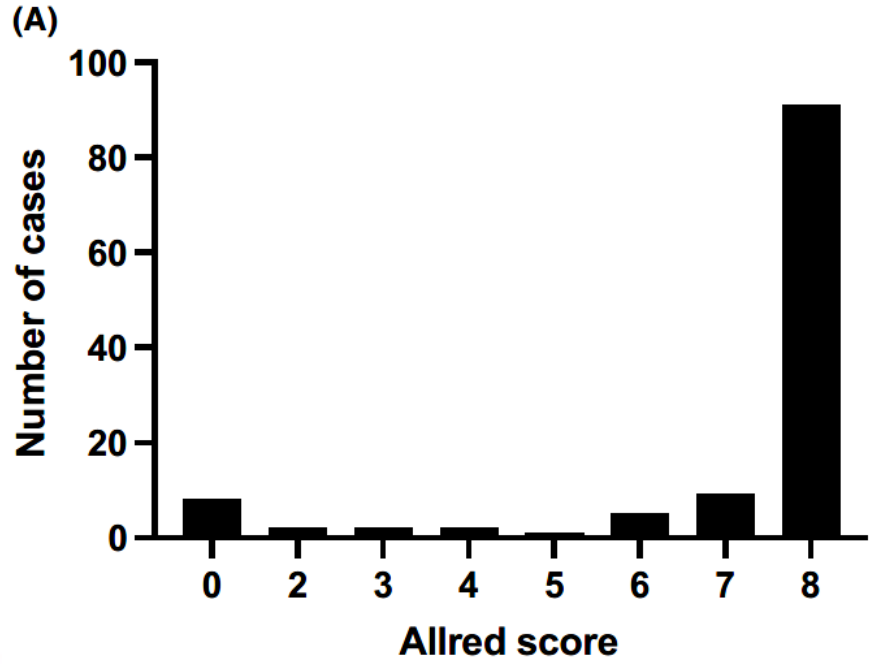

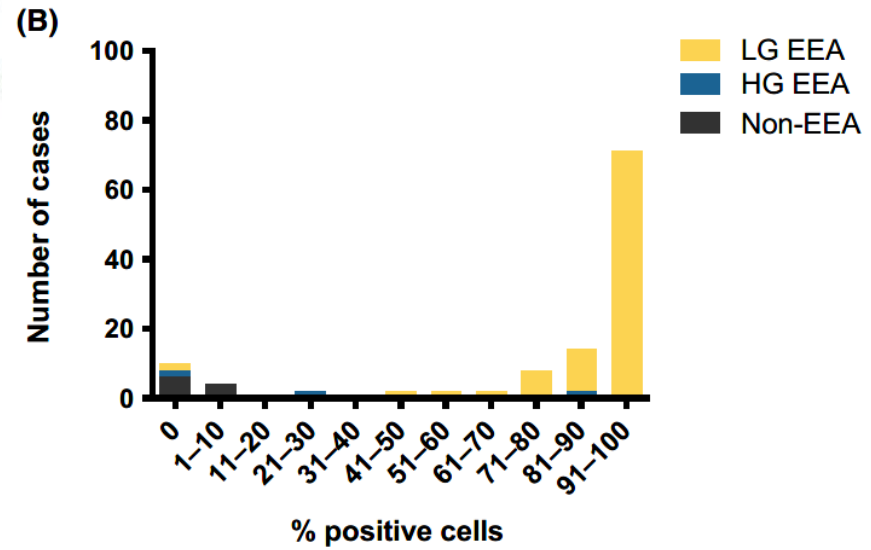

Clinicopathological and Molecular Characterization of High Grade Endometrial Carcinomas of No Specific Molecular Profile (NSMP) Stratified by ER Status

Patrick Thaddeus Timmermans, BSc, Alicia Leon-Castillo, MD, PhD,† Claire Kramer, BSc,* Natalja Ter Haar,* Vincentius Smit, MD, PhD,* Marie Boennelycke, MD, PhD,‡ Estrid Hogdall, MD, PhD,§ Claus Hogdall, MD, PhD,‖ Carien L. Creutzberg, MD, PhD,¶ Nanda Horeweg, MD, PhD,¶ Gitte Ortoft, MD, PhD,‖ and Tjalling Bosse, MD, PhD**

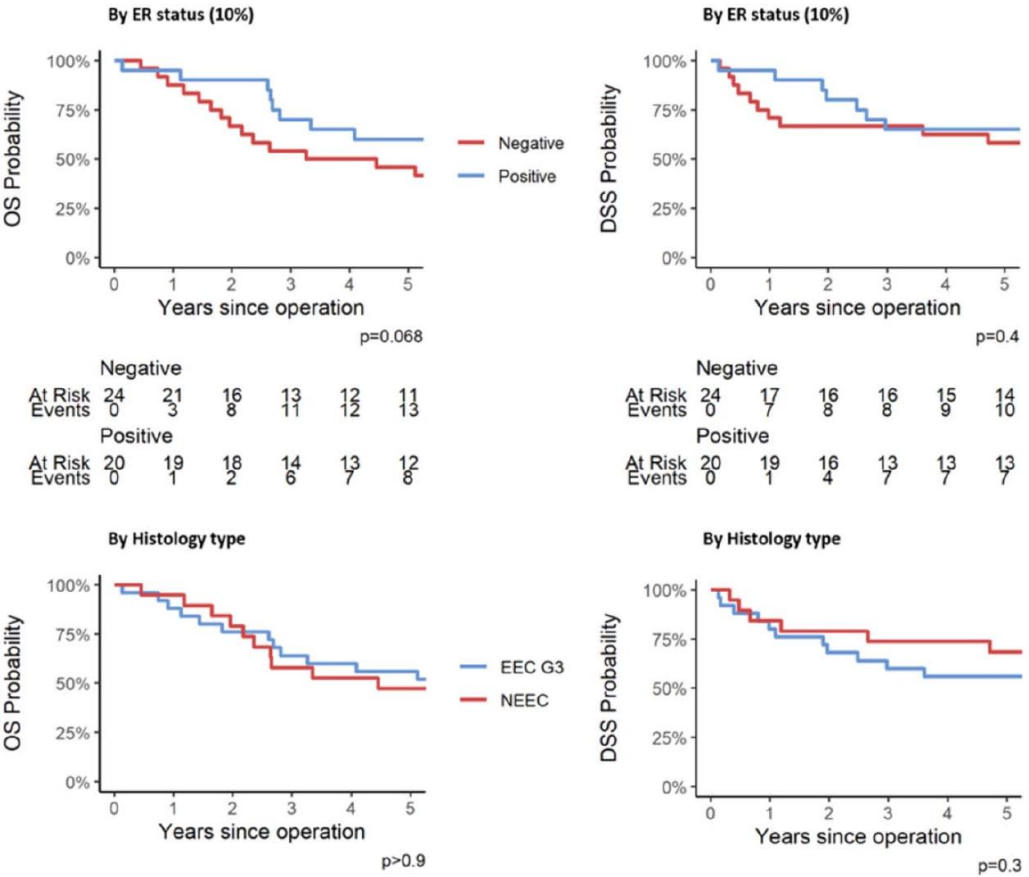

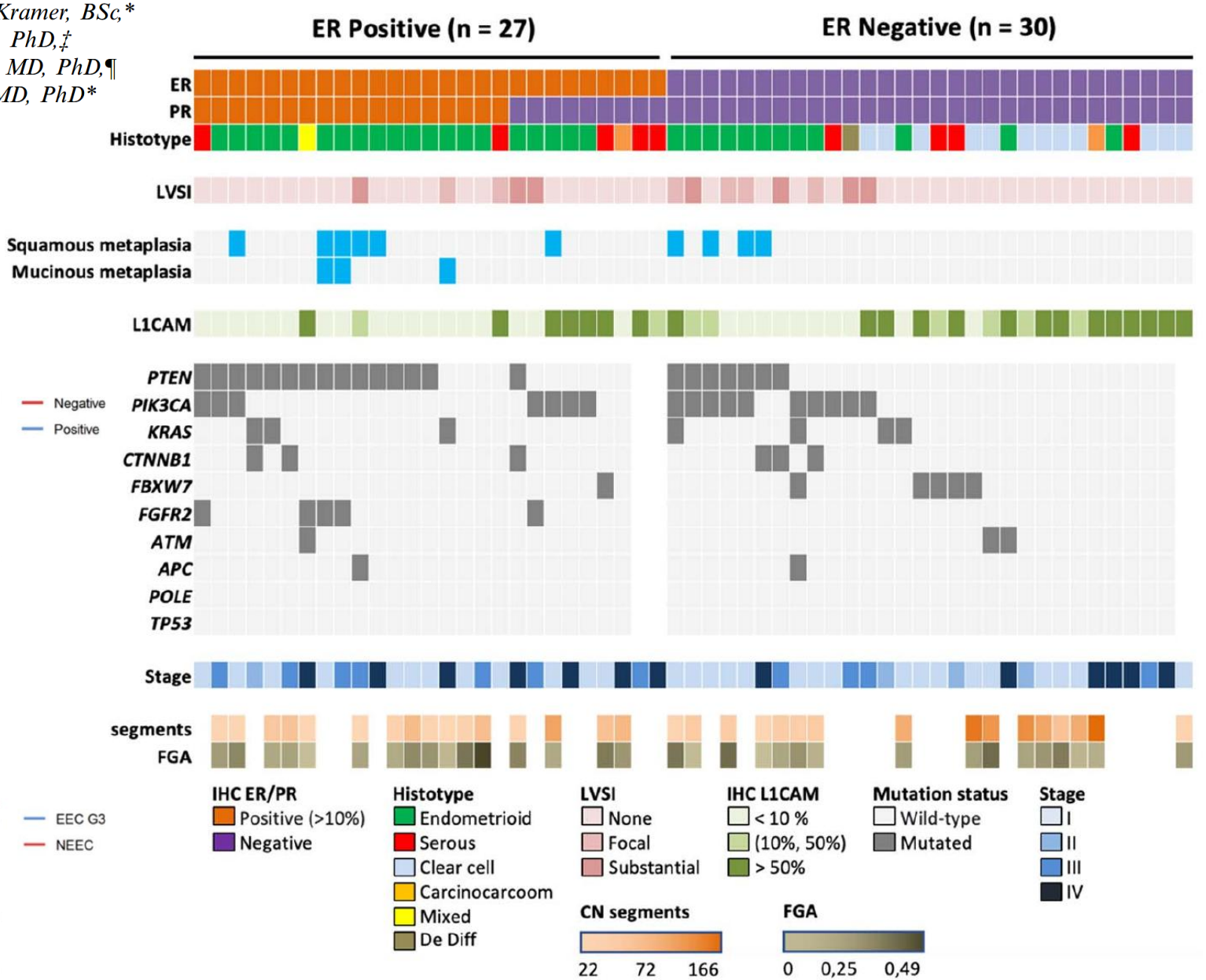

Endometrial carcinoma

- Molecular classification and Mullerian carcinosarcomas

Int J Gynecol Pathol 2024;43:506–514
Am J Surg Pathol 2024;48:953–964
Mod Pathol 2025;38:100676

- Carcinosarcoma with Mesonephric-like components

Am J Surg Pathol 2025;49:439–447

Molecular Classification Outperforms Histologic Classification in Prognostication of High-grade Endometrial Carcinomas With Undifferentiated and Sarcomatous Components

Phoebe M. Hammer, MD, Aihui Wang, ScM,* Lisa Vermij, PhD,† Sabrina Zdravkovic, BS,*
Lucas Heilbroner, BA,* Emily Ryan, MD,* Rachel L.P. Geisick, MLS (ASCP),*
Vivek Charu, MD, PhD,* Teri A. Longacre, MD,* Carlos J. Suarez, MD,*
Chandler Ho, MLS (ASCP), MB,* Taylor M. Jenkins, MD,‡ Anne M. Mills, MD,§
Tjalling Bosse, MD, PhD,† and Brooke E. Howitt, MD**

TABLE 1. Summary of Clinical, Histologic, and Molecular Features in the Cohort

Clinical and molecular features	Carcinosarcoma (n = 96)		DDEC/UDEC (n = 49)		GR3spEEC (n = 17)	
Molecular subtype	POLE = 4 (4.2%) MMRd = 11 (11.6%) P53abn = 63 (65.6%) NSMP = 18 (18.8%)		POLE = 7 (14.3%) MMRd = 27 (55.1%) P53abn = 8 (16.3% NSMP = 7 (14.3%)		POLE = 1 (5.9%) MMRd = 5 (29.4%) P53abn = 6 (35.3%) NSMP = 5 (29.4%)	
Predominant epithelial component	(n=69 evaluated) Endometrioid = 27 (39.1%) Serous = 20 (29%) Ambiguous/undifferentiated = 22 (31.9%) Unknown = 27		(n=32 evaluated) Endometrioid = 18 (56.3%) Ambiguous/ Undifferentiated = 13 (40.6%) Clear Cell = 1 (3.1%) Unknown = 17		(n=17 evaluated) Endometrioid = 17	
Heterologous differentiation	Total=28/71 (39%) Rhabdomyosarcomatous = 17 (60.7%) Chondrosarcomatous = 7 (25%) Osteosarcomatous = 1 (3.6%) Liposarcomatous = 1 (3.6%) Mixed = 2 (7.1%)		Total=1/35 (2.9%) Chondrosarcomatous = 1 (100%)		Total=0/17 (0%)	
FIGO stage	Stage I-II (n = 53)	Stage III-IV (n = 43)	Stage I-II (n = 27)	Stage III-IV (n = 22)	Stage I-II (n = 9)	Stage III-IV (n = 8)
Age at surgery (y), median	67 (25–85)	68.5 (47–91)	68 (35–81)	60 (28–79)	64 (43–84)	61.5 (34–78)
BMI, Median	29.3	25.4	33.6	30.3	29.9	34.6
Tumor size (cm), median	5.3 (1–17)	5.4 (1.2–17.2)	4.8 (3.3–10)	6.4 (1.1–15)	4.0 (3.5–7.2)	9.1 (3.5–14)
Lymph node involvement	0% (0/39)	72% (18/25)	0% (0/19)	55% (6/11)	0% (0/7)	75% (3/4)

DDEC/UDEC indicates Dedifferentiated/undifferentiated carcinoma; GR3spEEC, grade 3 endometrioid endometrial carcinoma with a spindled component.

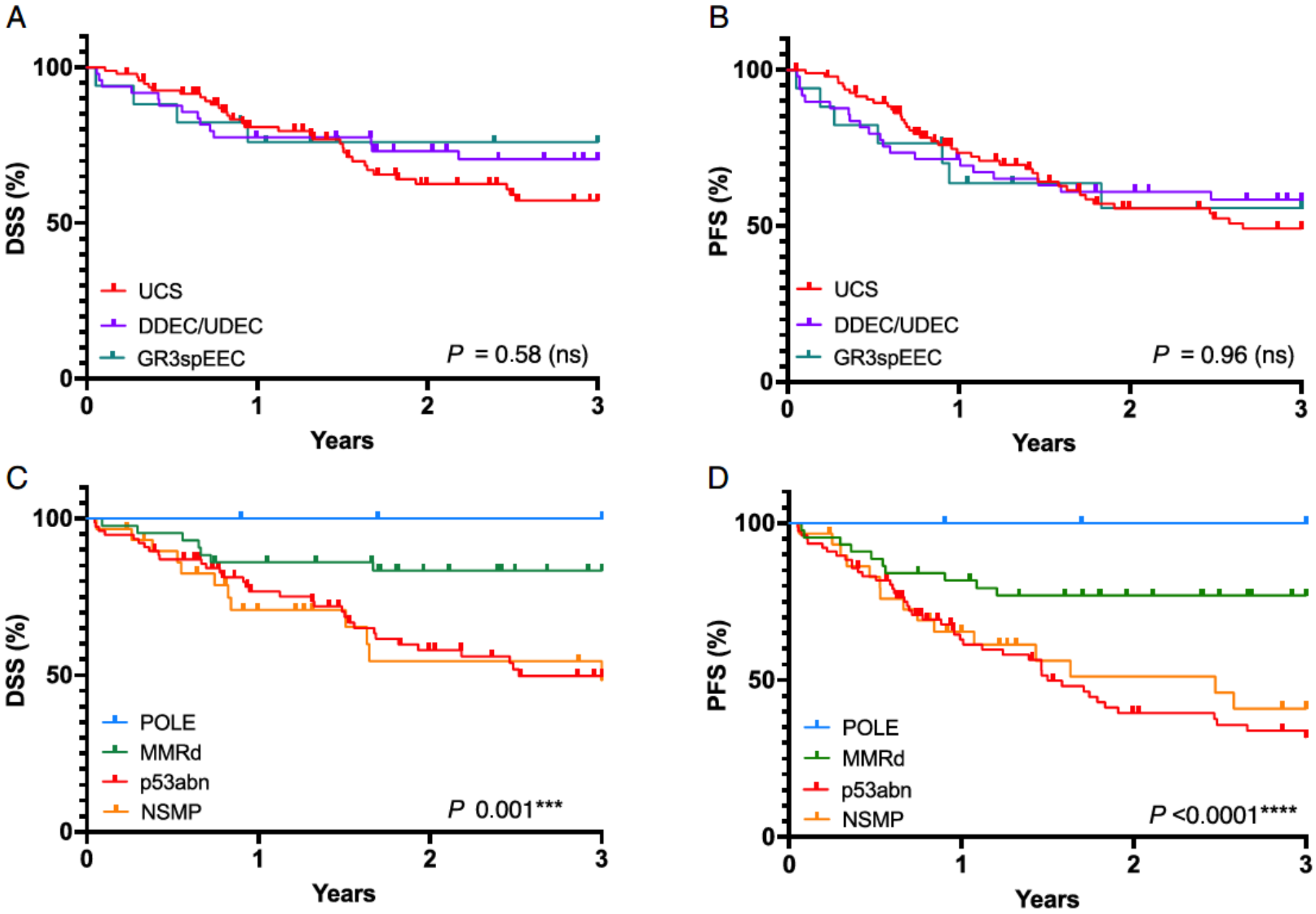
A
100
50
0
DSS (%)
UCS
DDEC/UDEC
GR3spEEC
P = 0.58 (ns)
0
1
2
3
Years
B
100
50
0
PFS (%)
UCS
DDEC/UDEC
GR3spEEC
P = 0.96 (ns)
0
1
2
3
Years
C
100
50
0
DSS (%)
POLE
MMRd
p53abn
NSMP
P 0.001***
0
1
2
3
Years
D
100
50
0
PFS (%)
POLE
MMRd
p53abn
NSMP
P <0.0001****
0
1
2
3
Years

POLE-Mutated Uterine Carcinosarcomas: A Clinicopathologic and Molecular Study of 11 Cases

Phoebe M. Hammer[a], Amir Momeni-Boroujeni[b], David L. Kolin[c], Leandra Kingsley[a], Ann Folkins[a], Rachel L.P. Geisick[a], Chandler Ho[a], Carlos J. Suarez[a], Brooke E. Howitt[a,*]

(n = 2) was observed. Mean and median follow-ups were 24.3 and 14.1 months, respectively (range, 1.4-61.1 months). Ten patients (91%) had no recurrences or death from disease, although 3 of these had follow-up periods <1 year. One patient, with the subclonal *POLE* variant, presented with stage IV disease and died 1.4 months after surgery. In conclusion, *POLE*mut UCS demonstrate unique

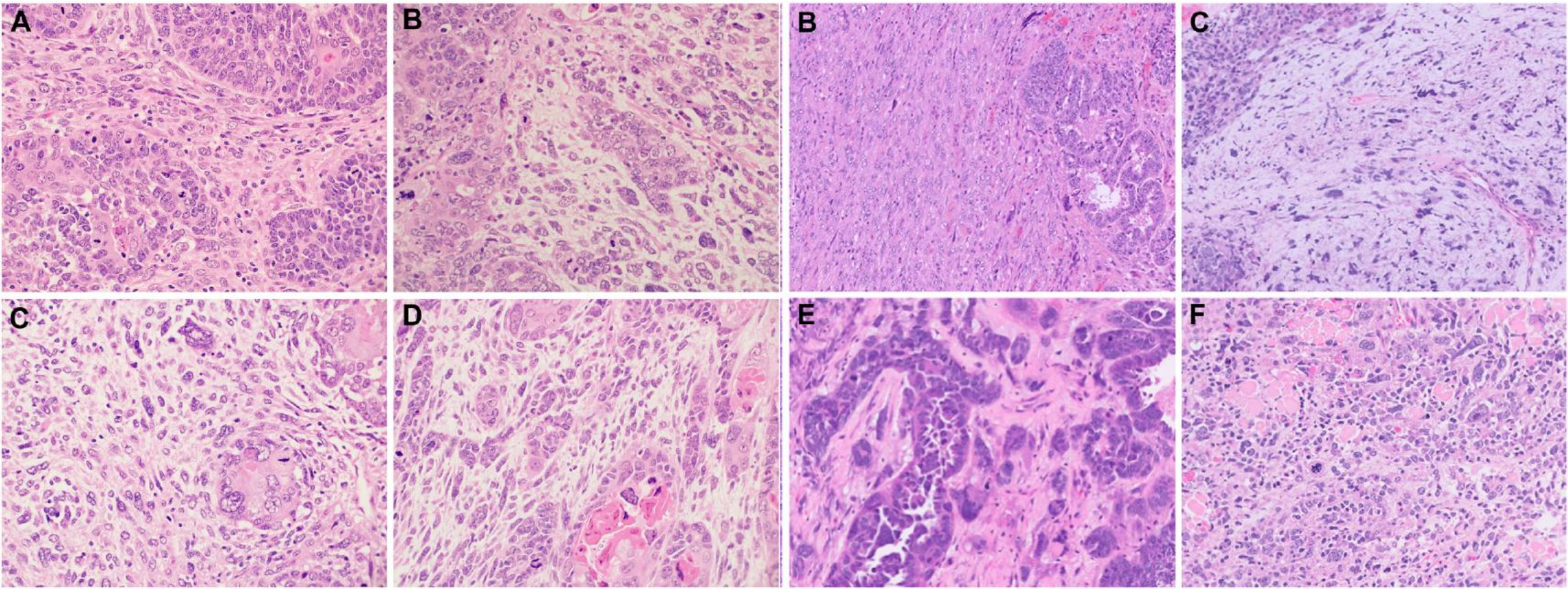

BACK

Endometrial Carcinosarcomas are Almost Exclusively of p53abn Molecular Subtype After Exclusion of Mimics

Jutta Huvila, M.D., P.h.D., Amy Jamieson, M.B.Ch.B, Jennifer Pors, M.D., Lynn Hoang, M.D., Jelena Mirkovic, M.D., Dawn Cochrane, Ph.D., Jessica N. McAlpine, M.D., and C. Blake Gilks, M.D.

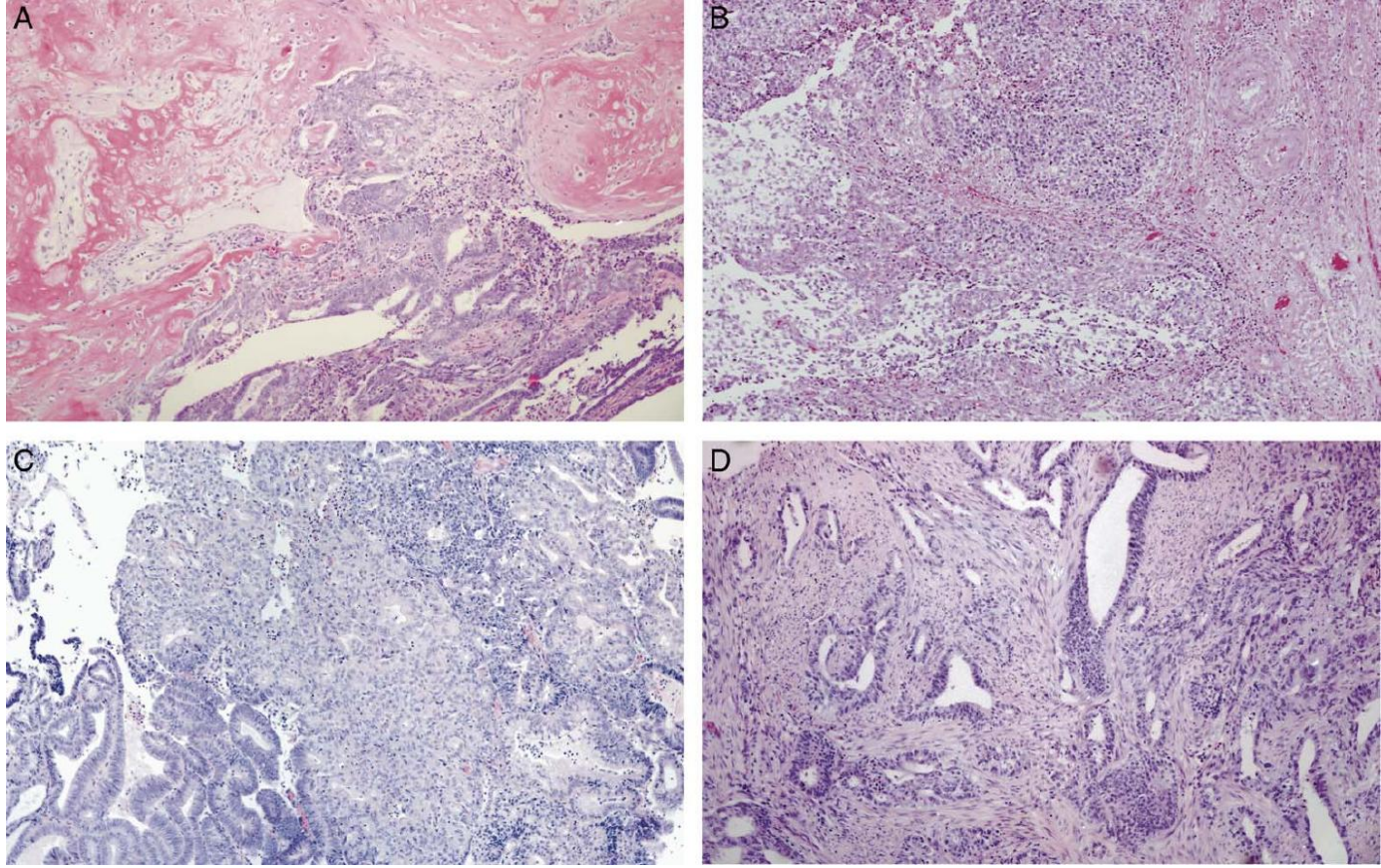

In the 2016 cohort, 37 of the 41 carcinosarcomas (91.2%) were p53abn, 2 (4.9%) were NSMP, and 1 each (2.4%) were *POLE*mut and mismatch repair deficiency molecular subtypes, respectively. Of the 4 non-p53abn tumors on review, both NSMP tumors were corded and hyalinized (CHEC) pattern endometrioid carcinoma, the mismatch repair deficiency tumor was a grade 1 endometrioid carcinoma with reactive stromal proliferation, and the *POLE*mut tumor was grade 3 endometrioid carcinoma with spindle cell growth, that is, none were confirmed to be carcinosarcoma on review.

Clinicopathologic and Molecular Characterization of Gynecologic Carcinosarcomas With a Mesonephric-Like Carcinomatous Component

Rachelle P. Mendoza, MD, Melisa Y. Tjota, MD, PhD,† Donghyuk N. Choi, BS,‡ David B. Chapel, MD,§ David L. Kolin, MD, PhD,‖ Elizabeth D. Euscher, MD,¶ Julieta E. Barroeta, MD,† Tricia A. Numan, MD,# Deyin Xing, MD, PhD,# Michelle Afkhami, MD,** Rania Bakkar, MD,** and Ricardo R. Lastra, MD†*

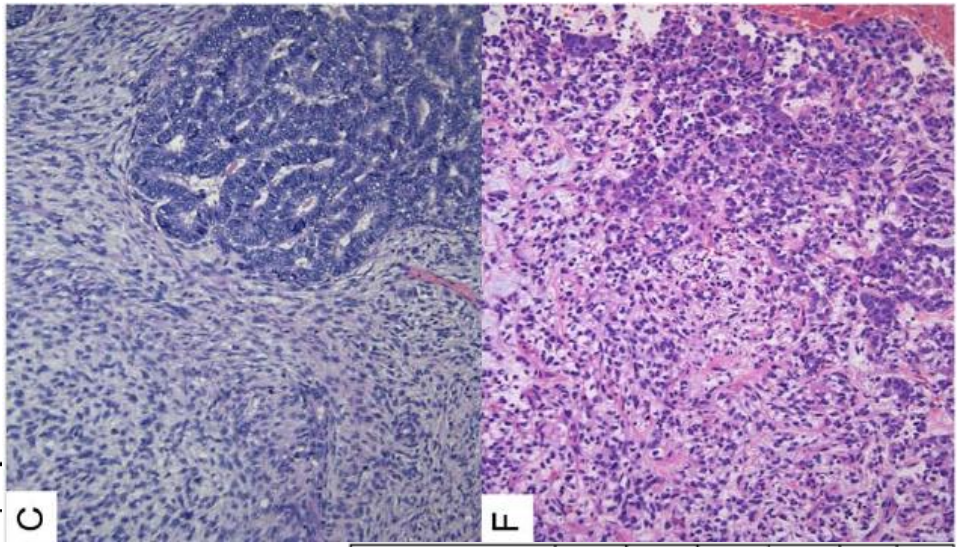

TABLE 1. Clinicopathologic Features of Mesonephric-Like Carcinosarcoma

Case	Age (y)	Size (cm)	FIGO stage	Tumor location	LVI	Presence of mesonephric remnants	Uterine serosa involvement	Cervical stroma involvement	Sarcomatous component	Location of metastatic or recurrent disease	Treatment	up period (mo)	at last follow-up
1	64	4	IIIA	Endometrium	Absent	Not identified	Present	Absent	Sarcoma, NOS	None	Chemotherapy, radiation	35	AWD
2	74	6.1	IB	Endometrium	Absent	Not identified	Absent	Absent	Sarcoma, NOS	None	Chemotherapy, radiation	17	NED
3	50	9.5	IB	Ovary	Absent	Not identified	Absent (ovarian surface involvement present)	Not applicable	Sarcoma, NOS, and heterologous (chondrosarcoma)	Peri-ureteral masses at 24 months (carcinoma)	Chemotherapy	30	NED
4	58	Unknown	II	Lower uterine segment	Absent	Not identified	Absent	Present	Sarcoma, NOS	Abdominal wall at 9 months (carcinoma), port site at 18 months (carcinoma), abdominal wall at 24 months (carcinoma), small bowel at 54 months (carcinoma and sarcoma)	Chemotherapy, radiation	58	AWD
5	83	3.5	II	Lower uterine segment	Present (focal)	Not identified	Absent	Present	Sarcoma, NOS, and heterologous (rhabdomyoblasts)	None	Radiation	52	NED
6	57	12	IV	Endometrium	Absent	Not identified	Absent	Present	Sarcoma, NOS, and heterologous (chondrosarcoma)	Lung	Chemotherapy, immunotherapy	36	DOD
7	62	15	IIIA	Endometrium	Present (focal)	Not identified	Present	Absent	Sarcoma, NOS	Lung, right fallopian tube at 4 months	Chemotherapy	13	DOD
8	77	9	1A	Endometrium	Present (extensive)	Not identified	Absent	Absent	Sarcoma, NOS, and heterologous (chondrosarcoma)	None	Chemotherapy	5	NED

AWD indicates alive with disease; DOD, dead of disease; LVI, lymphovascular invasion; NED, alive, no evidence of disease.

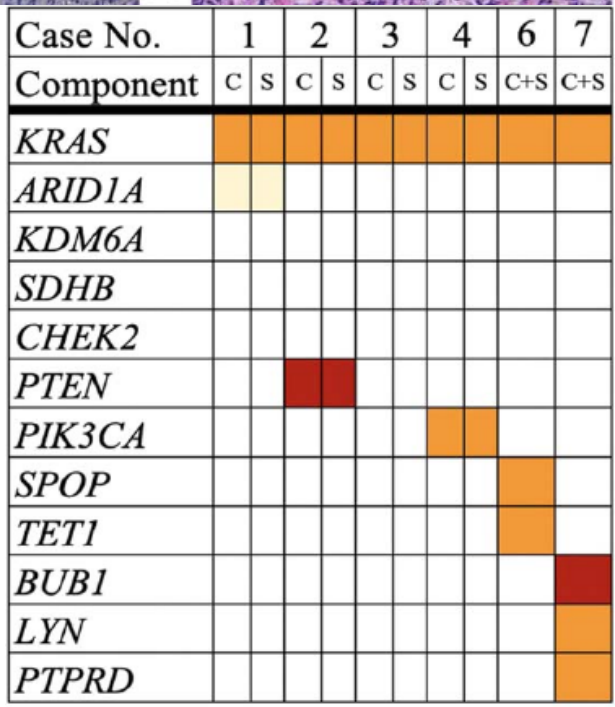

C = carcinomatous component
S = sarcomatous component

Uterine mesenchymal lesions

- PLAG-1 rearranged sarcoma

Mod Pathol 2024;37(9):100552

- Uterine leiomyosarcoma associated with PEComa

Am J Surg Pathol 2024;48:761–772

- P16 as surrogate of *CDKN2A* deletion in uterine IMT

Am J Surg Pathol 2024;48:813–824

PLAG1-Rearranged Uterine Sarcomas: A Study of 11 Cases Showing a Wide Phenotypical Spectrum Not Limited to Myxoid Leiomyosarcoma-Like Morphology

Michael Michal[a,b,*], Abbas Agaimy[c], Sabrina Croce[d], Gunhild Mechtersheimer[e], John M. Gross[f], Deyin Xing[f], Debra A. Bell[g], Sounak Gupta[g], Elaheh Mosaieby[a,b], Petr Martínek[a], Natálie Klubíčková[a,b], Květoslava Michalová[a,b], Jiří Bouda[h], Jindřich Fínek[i], Tahyna Hernandez[j], Michal Michal[a,b], J. Kenneth Schoolmeester[k], Ondrej Ondič[a,b]

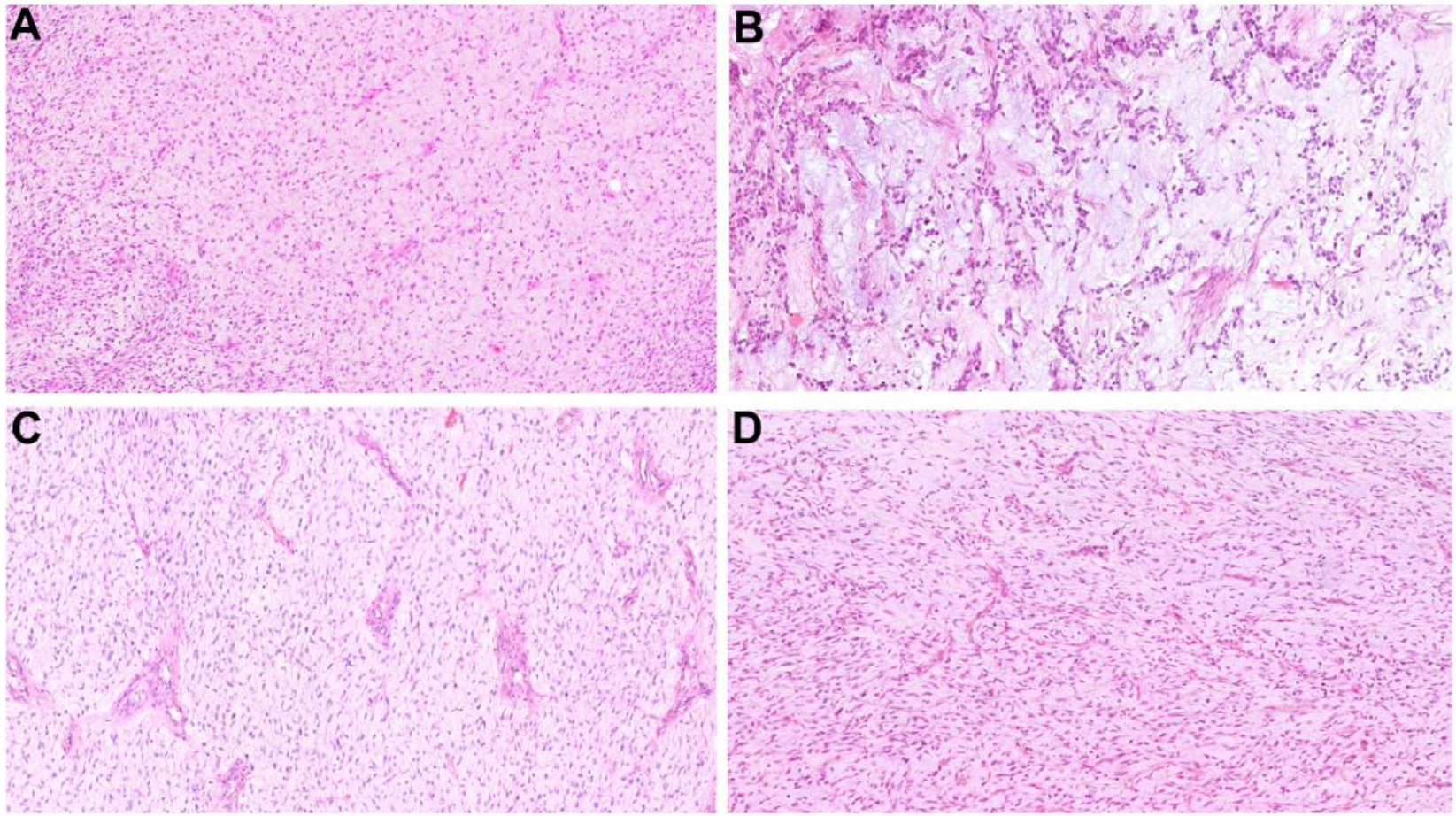

Figure 1.
Myxoid leiomyosarcoma–like morphology was present in only 3 of the primary tumors: case 2 (A) and case 8 (B). Case 1 (C) and case 7 (D) showed such areas in the metastases.

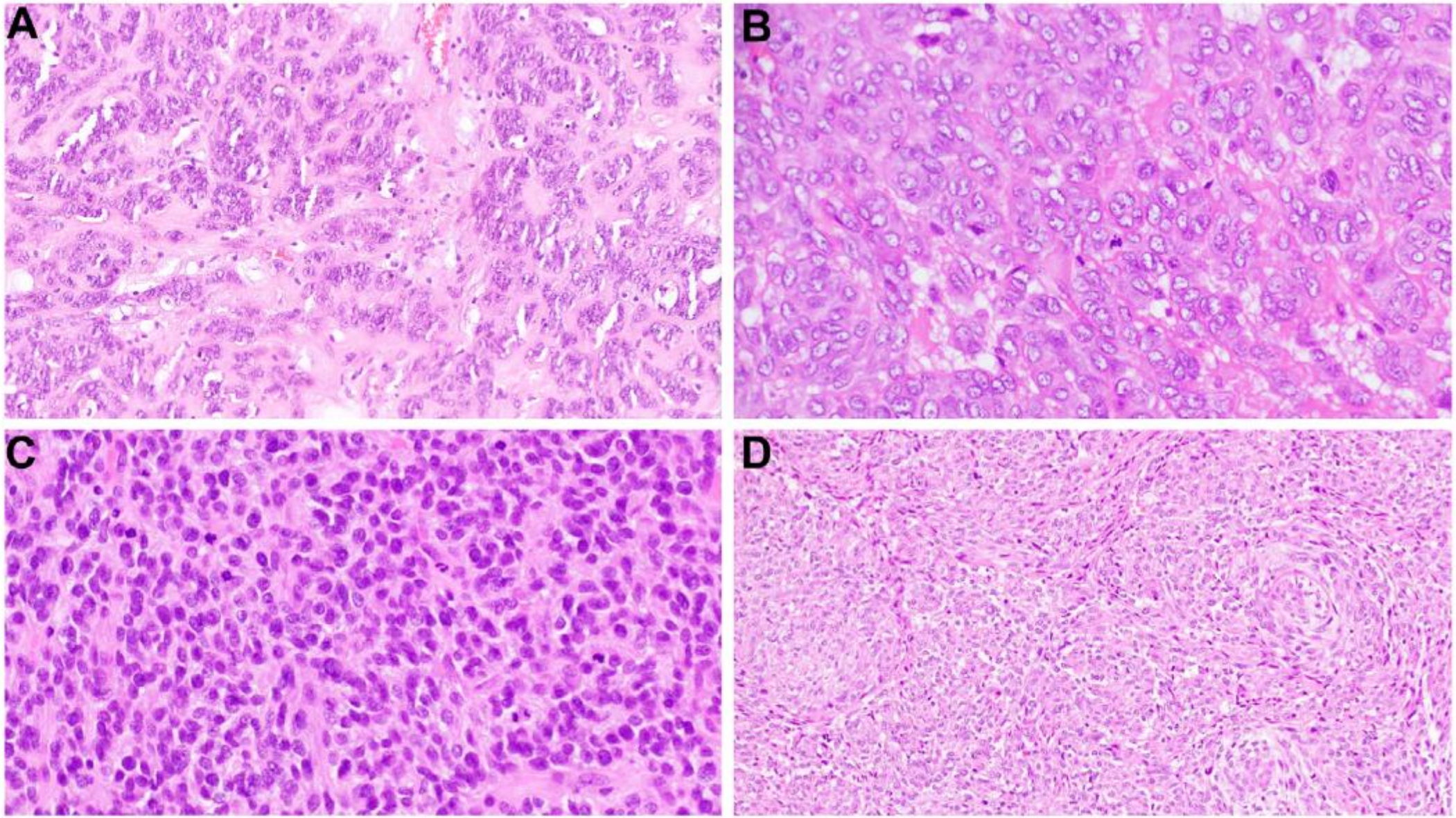

Figure 2.
Five cases presented with morphology consistent with epithelioid leiomyosarcoma: (A) case 9, (B) case 5, (C) case 4, and (D) case 3.

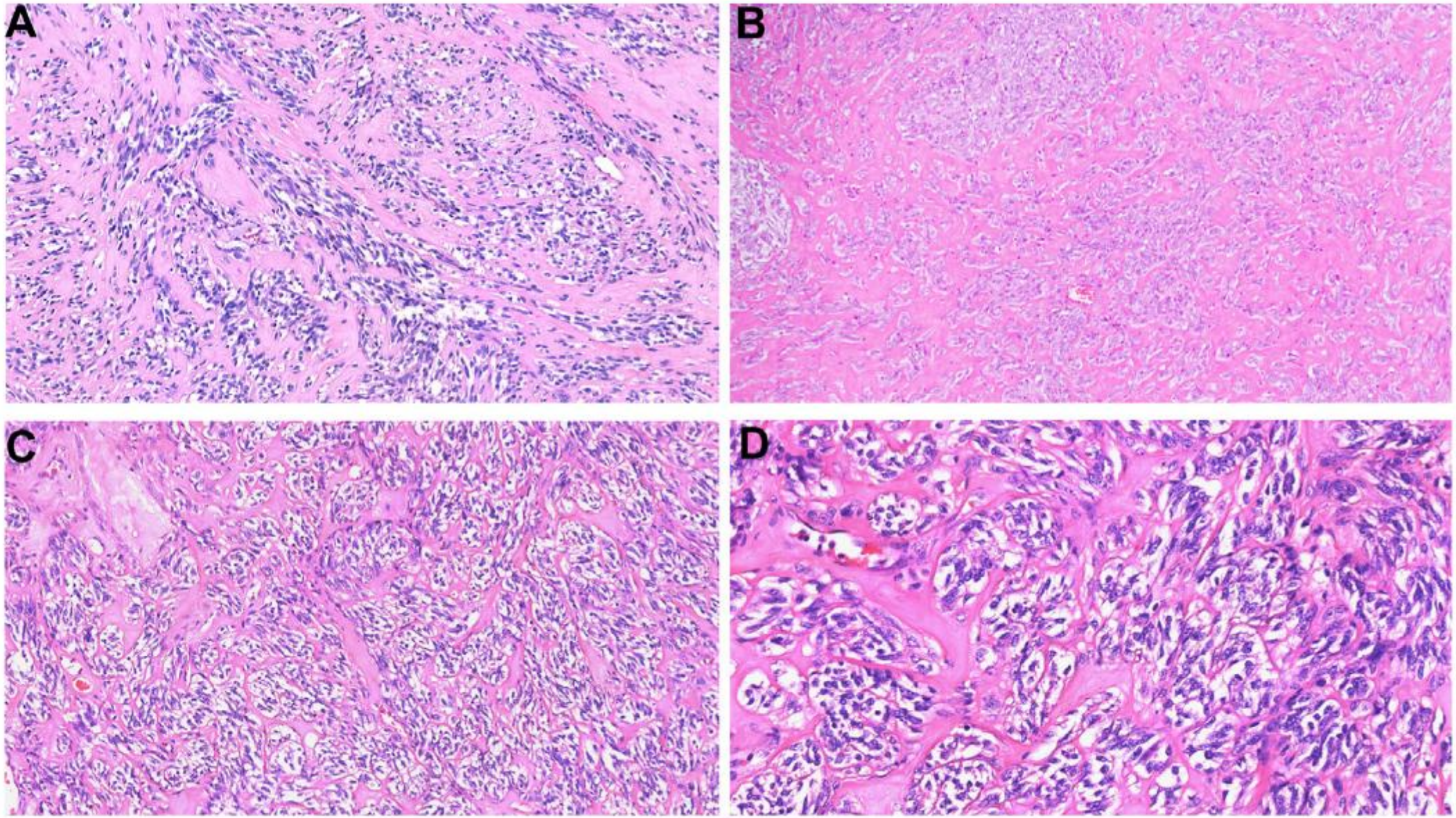

Figure 4.
Three cases featured areas with prominently hyalinized stroma dividing the lesion into variably sized nests: (A) case 1, (B) case 5, and (C and D) case 9.

BACK

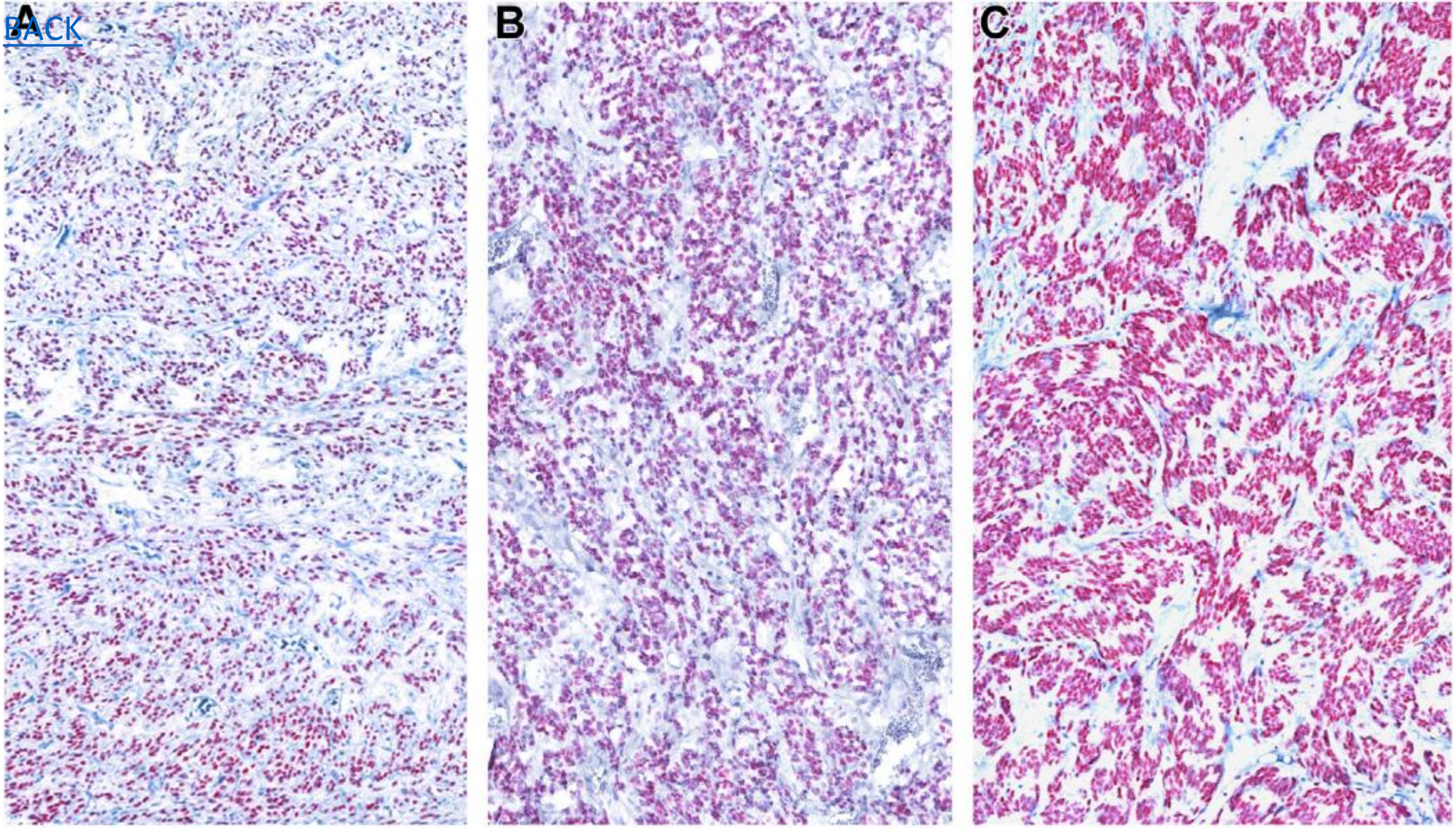

Uterine Leiomyosarcoma Associated With Perivascular Epithelioid Cell Tumor

A Phenomenon of Differentiation/Dedifferentiation and Evidence Suggesting Cell-of-Origin

Levon Katsakhyan, MD, Maryam Shahi, MD,* Henrietta C. Eugene, BS,* Hiro Nonogaki, MS,* John M. Gross, MD,* Marisa R. Nucci, MD,† Russell Vang, MD,*‡ and Deyin Xing, MD, PhD*‡§*

TABLE 1. Clinicopathological Features

Case	Age (y)	Clinical presentation	Surgical procedure	Tumor site and size	Smooth muscle tumor (%)	PEComa component (%)	Follow-up
1	75	Postmenopausal bleeding and uterine mass	TH-BSO, lymph node dissection	Submucosa: 4.0 cm	LMS (90%)	Differentiation; uncertain malignant potential (10%)	Recent case
2	73	Postmenopausal bleeding and thickened endometrial stripe	TH-BSO, omentectomy, lymph node dissection, staging biopsies	Uterine corpus: 3.0 cm	LMS (60%)	Dedifferentiation; malignant (40%)	36 mo; multiple bone metastases
3	76	Postmenopausal bleeding and uterine mass	TH-BSO, omentectomy	Uterine corpus: 11.5 cm	LMS (20%)	Dedifferentiation; malignant (80%)	12 mo; dead of disease
4	63	Postmenopausal bleeding and uterine mass	TH-BSO, omentectomy	Uterine corpus: 9.5 cm	LMS (70%)	Differentiation/ dedifferentiation; malignant (30%)	45 mo; no evidence of disease

BACK

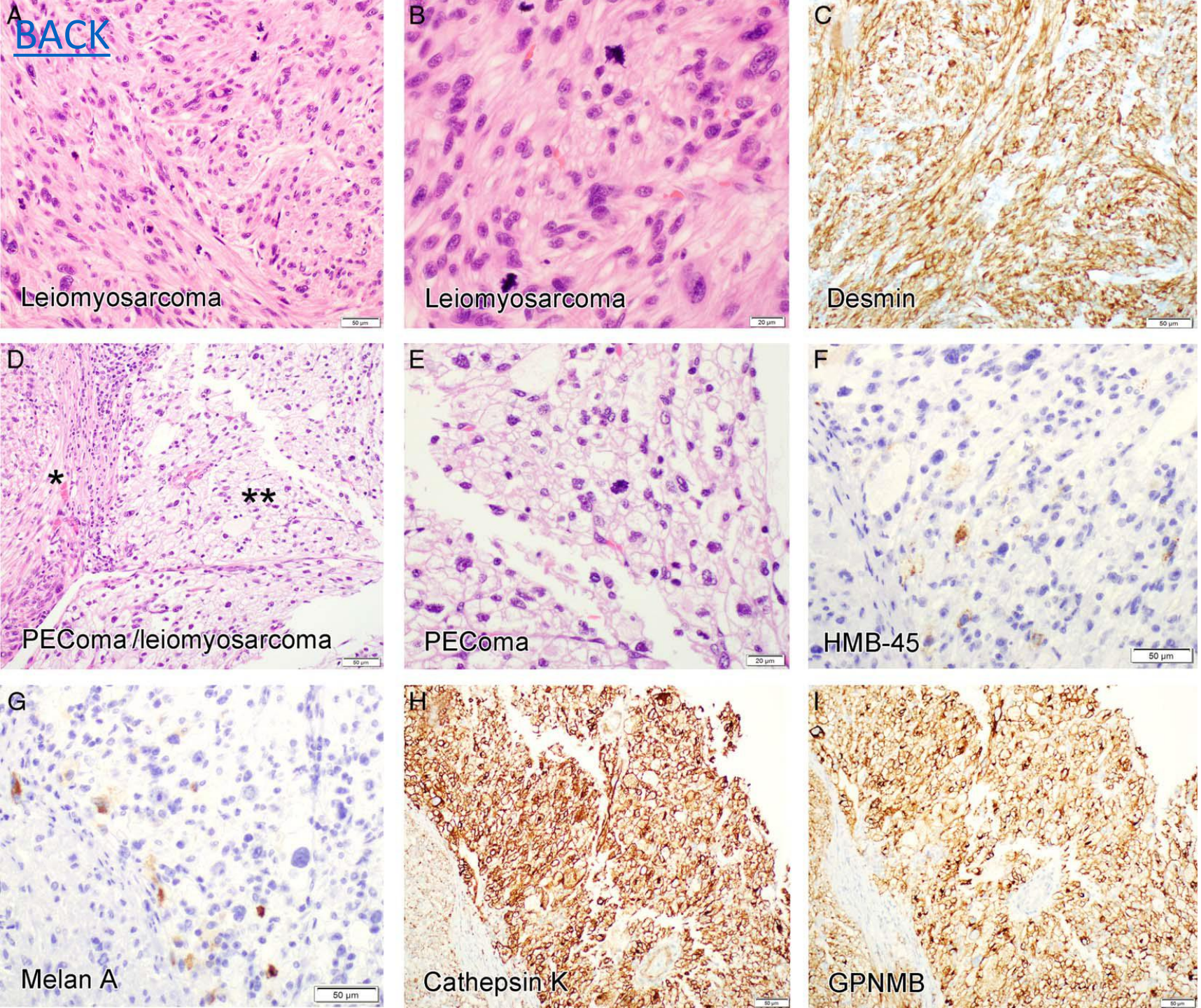

- LMS component
  - Diffuse desmin
  - Neg HMB45 / Melan-A
  - Focal Cathepsin K
- PEComa component
  - Focal HMB45 / Melan-A
    Diffuse Cathepsin K
- Shared events:
  - FH loss (case 1)
  - Rb1 loss (case 2-4)
  - P53 null (cases 2 & 3)
  - TP53 p.R196* (case 2)

Uterine Inflammatory Myofibroblastic Tumors

p16 as a Surrogate for CDKN2A Deletion and Predictor of Aggressive Behavior

Kyle M. Devins, MD, Zehra Ordulu, MD,† Rachelle P. Mendoza, MD,‡ Sabrina Croce, MD, PhD,§ Rishikesh Haridas, MS,‖ Pankhuri Wanjari, MS,‖ Andre Pinto, MD,¶ Esther Oliva, MD,* and Jennifer A. Bennett, MD‖*

Am J Surg Pathol 2023;47:157-171

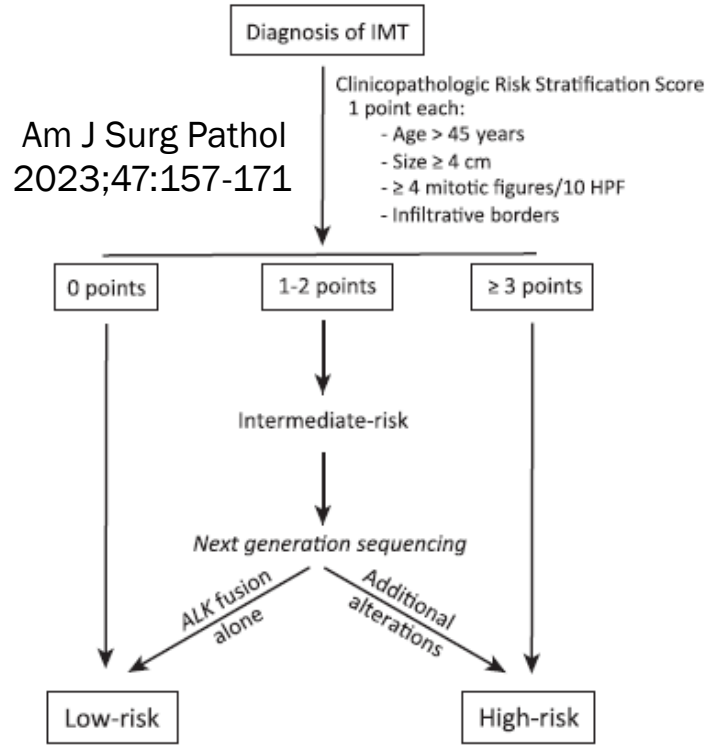

FIGURE 6. Proposed 2-step risk stratification model for predicting clinical behavior of uterine IMT.

Application of the previously described clinicopathologic risk stratification score in all primary IMTs with complete data (n = 18) classified 8 as high-risk (all malignant), 8 as intermediate-risk (3 malignant, 5 benign), and 2 as low-risk (benign). p16 was aberrant in all malignant IMTs, with < 1% expression noted in 10, overexpression (> 90%) in 4, and subclonal loss in 1; all benign tumors had patchy staining

The most effective prognostic tool in our cohort was p16 immunohistochemistry. All malignant IMTs demonstrated aberrant p16 expression, while all benign tumors showed patchy staining. Thus, our findings support the use of p16 as an independent predictive marker in uterine IMTs

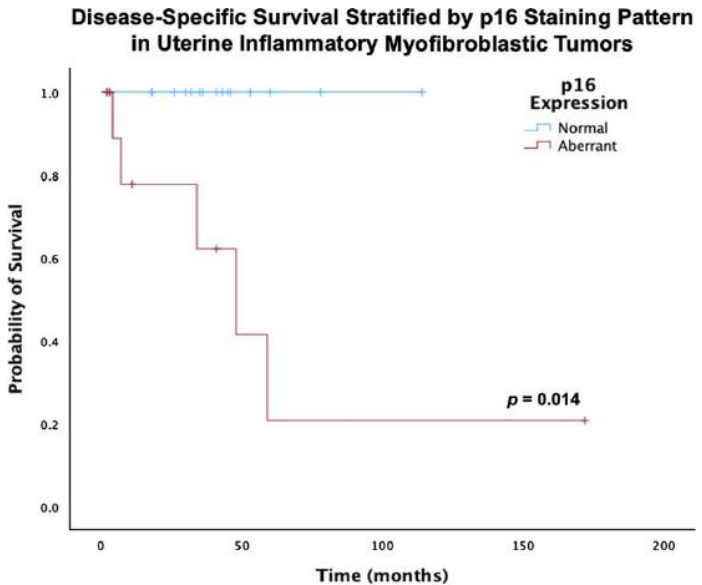

Trophoblastic disease

- Distinction between diandric vs digyinic triploid gestations

Histopathology 2024, 85, 879–888

- SALL4 immunohistochemistry in Dx of choriocarcinoma and complete hydatidiform mole vs mimics

Am J Surg Pathol 2025;49:417–428

Diandric triploid partial mole versus digynic nonmolar triploidy: is morphological assessment sufficient for the diagnostic distinction?

Agnes Nagy,[1] Na Niu,[2,3] Tong Sun,[2] Natalia Buza[2,3] & Pei Hui[2,3]
[1]*Department of Pathology and Experimental Cancer Research, Semmelweis University, Budapest, Hungary,*
[2]*Department of Pathology and* [3]*Center for the Precision Medicine of Trophoblastic Disease, Yale School of Medicine, New Haven, CT, USA*

Conclusions: None of histological parameters are unique to either diandric triploid gestation or digynic triploid gestation. Cistern formation is the most powerful discriminator, with 93% PPV and 70% sensitivity for diandric triploid gestation. While cistern formation combined with either trophoblastic hyperplasia or villous size ≥2.5 mm or syncytiotrophoblast lacunae has 100% PPV and specificity for diandric triploid gestation, the sensitivity is only 60% to 65%. Therefore, in the presence of triploidy, histological assessment is unable to precisely classify 35% to 40% of diandric triploid gestations or partial moles.

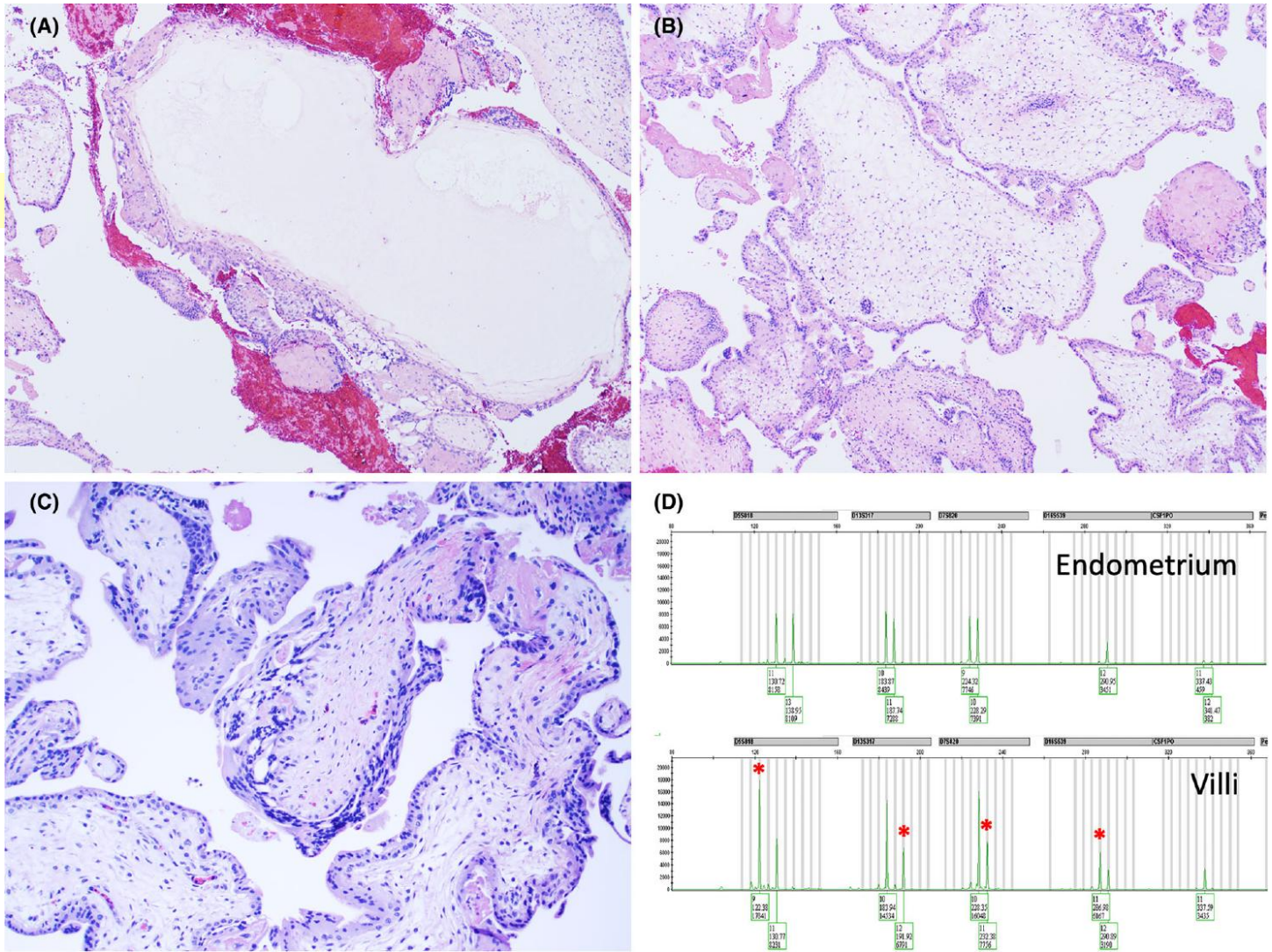

BACK

Histological parameters (single or combined)	PHM (N = 20)	DTG (N = 22)	Sensitivity %	Specificity %	PPV %	P value
Single parameters						
Cistern formation	14	1	70	96	93	<0.00001
Trophoblast hyperplasia	14	2	70	91	88	0.00005
Syncytiotrophoblast lacunae	18	4	90	82	82	<0.00001
Villous size ≥2.5 mm	15	5	75	77	75	0.00075
Trophoblast atypia	5	2	25	91	71	0.167
Villous hydrops (at least moderate)	18	8	90	64	69	0.0035
Presence of foetal parts	11	5	55	77	69	0.0315
Syncytiotrophoblast knuckles	19	13	95	41	59	0.0064
Two villous populations	14	13	70	41	52	0.461
Trophoblastic pseudoinclusions	18	18	90	18	50	0.449
Irregular villous shape and/or contour	19	21	95	4.5	48	0.945
Blood vessels	17	21	85	4.5	45	0.249
Nucleated foetal red blood cells	15	20	75	9	41	0.167
Presence of calcifications	9	17	45	23	35	0.0315
Single cell trophoblast inclusions	5	10	25	55	33	0.167
Combined parameters						
Cistern + villous size ≥2.5 mm	12	0	60	100	100	
Cistern +trophoblast hyperplasia	12	0	60	100	100	
Cistern + Syncytiotrophoblast lacunae	13	0	65	100	100	
Syncytiotrophoblast Lacunae + trophoblast hyperplasia	13	1	65	96	93	
Villous size ≥2.5 mm + lacunae	18	2	90	91	90	
Villous size ≥2.5 mm + trophoblast hyperplasia	10	2	50	91	83	

DTG, digynic triploid gestation; PHM, partial hydatidiform mole; PPV, positive predictive value.

SALL4 as a Useful Marker for the Distinction of Various Gestational Trophoblastic Disease Subtypes

Choriocarcinoma From Other Trophoblastic Lesions and Early Complete Hydatidiform Mole From Partial Mole and NonMolar Villi

Alexis Trecourt, MD,† Marie Donzel, MD,*‡ Lucie Gaillot-Durand, MD,*§*
Pierre A. Bolze, MD, PhD,§‖ François Golfier, MD, PhD,§‖ Pierre Descargues, MD,§‖
Touria Hajri, PhD,§ Claire Mauduit, PharmD, PhD,¶*
Mojgan Devouassoux-Shisheboran, MD, PhD,†§# and Fabienne Allias, MD*§*

SALL4 immunostaining was always negative in the syncytiotrophoblast of all GTD and nonmolar POC, while in cytotrophoblast/intermediate trophoblast SALL4 expression varied according to the histologic type of GTD

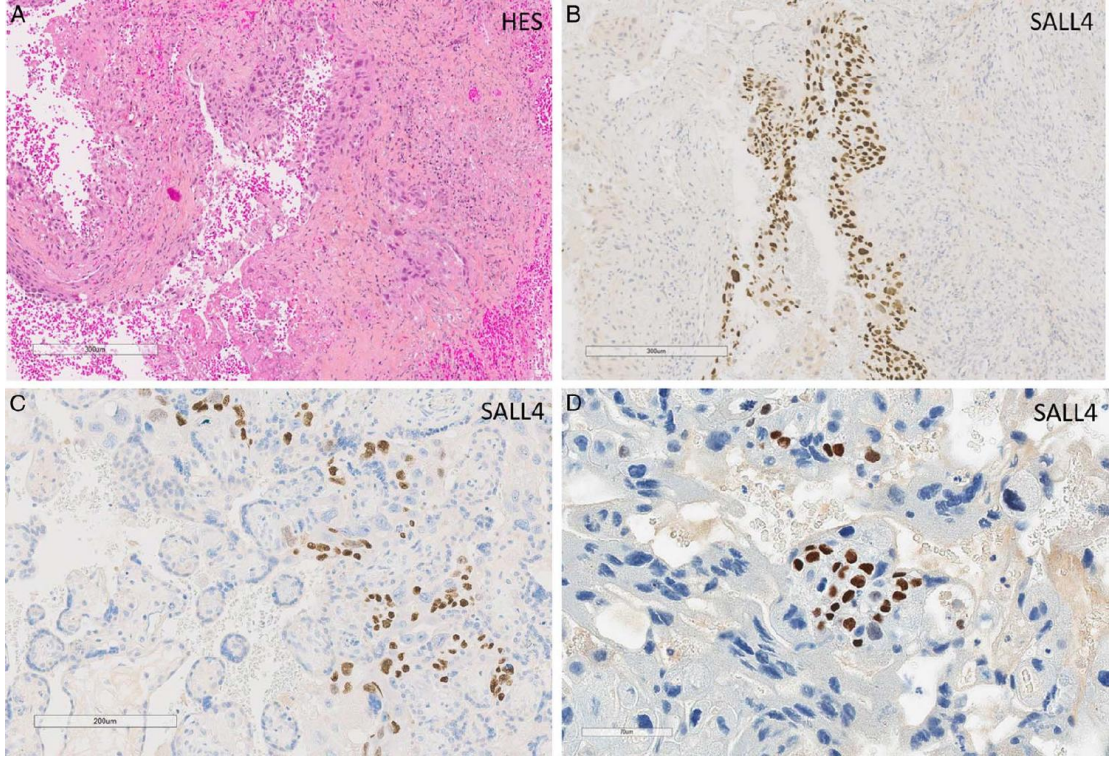

TABLE 2. Results of SALL4 Immunostaining in Cytotrophoblast/Intermediate Trophoblast

SALL4 expression in cytotrophoblast/intermediate trophoblast (%, n/N)	(0%)	(1%-10%)	(11%-100%)
CHM/IM (n = 47)	59.6 (28/47)	40.4 (19/47)	0 (0/47)
PHM (n = 13)	92.3 (12/13)	7.7 (1/13)	0 (0/13)
Nonmolar POC (n = 26)	96.3 (25/26)	1.7 (1/26)	0 (0/26)
PSN (n = 10)	100 (10/10)	0 (0/10)	0 (0/10)
APSN (n = 8)	100 (8/8)	0 (0/8)	0 (0/8)
ETT (n = 5)	100 (5/5)	0 (0/5)	0 (0/5)
PSTT (n = 9)	66.7 (6/9)	33.3 (3/9)	0 (0/9)
Choriocarcinoma (n = 31)	9.8 (3/31)	16.1 (5/31)	74.2 (23/31)

APSN indicates atypical placental site nodule; CHM/IM, complete hydatidiform mole /invasive mole; ETT, epithelioid trophoblastic tumor; PHM, partial hydatidiform mole; POC, products of conception; PSN, placental site nodule; PSTT, placental site trophoblastic tumor.

Upper Genital Serous Neoplasia

- High-grade anaplastic transformation of ovarian serous borderline tumour

Am J Surg Pathol 2024;48:1395–1407

- High-grade serous CA originating from Low-grade serous CA

Mod Pathol 2025;38:100629

High-grade Anaplastic Transformation of Ovarian Serous Borderline Tumor

A Distinctive Morphology With Abundant Dense Eosinophilic Cytoplasm and Dismal Prognosis

Xiaoming Zhang, MD, Kelly A. Devereaux, MD, PhD,*† Emily Ryan, MD,*‡ Fei Fei, MD,*§ Christian A. Kunder, MD, PhD,*‖ and Teri A. Longacre, MD**

We report the clinicopathologic features of seven SBTs, each associated with the presence of a morphologically unique high-grade component with an extremely dismal prognosis. All of the SBTs exhibited typical hierarchical branching and scattered eosinophilic cells, whereas the high-grade component consisted of a profuse proliferation of epithelioid cells with abundant dense, eosinophilic cytoplasm, variable nuclear pleomorphism, and evident loss of WT1, estrogen receptor, and p16 positivity. In most cases, the SBT demonstrated an abrupt transition to the high-grade component, but one patient initially presented with the usual SBT and developed a recurrent disease that was composed entirely of the high-grade component. Targeted next-generation sequencing revealed identical driver mutations in both the SBT and high-grade components (*BRAF* in 3, *KRAS* in 1), confirming clonality. Three cases, in addition, harbored telomerase reverse transcriptase promoter mutations in both components. One case, despite insufficient material for sequencing, was BRAF V600E-positive by immunohistochemistry. Most patients with available follow-up data died within 9 months of diagnosis.

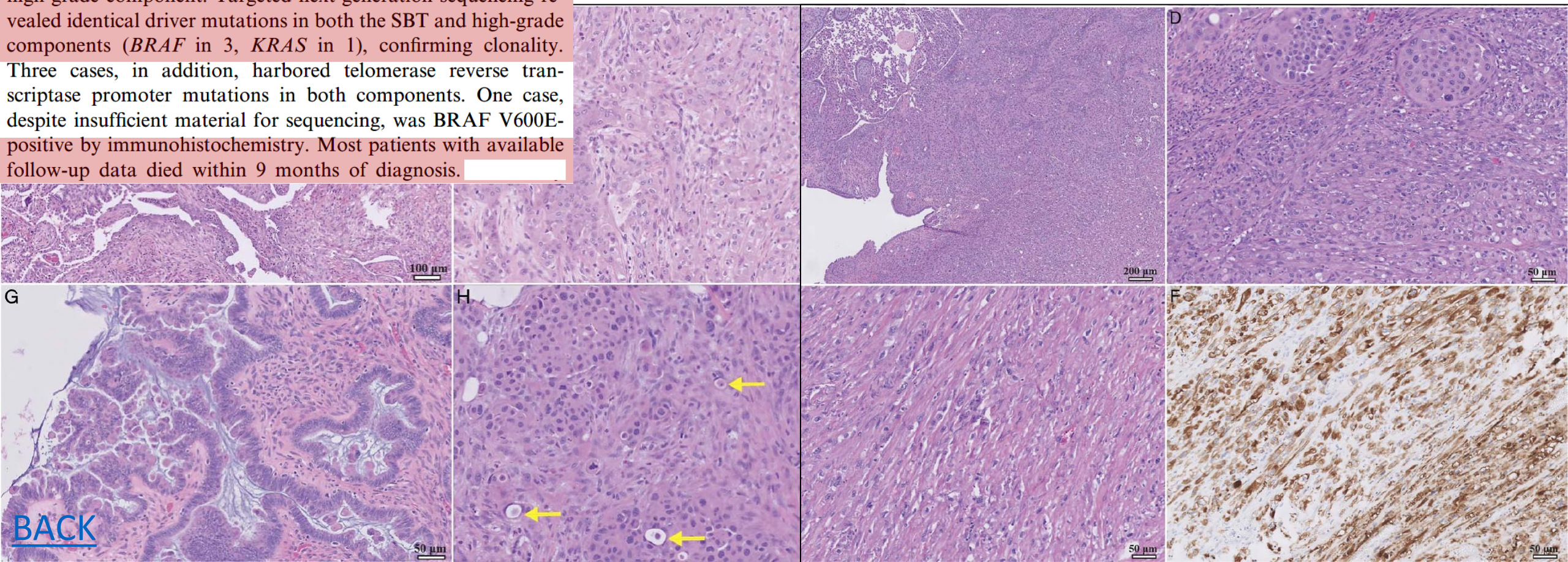

BACK

Early Genetic Divergence of High-Grade Carcinomas Originating from Low-Grade Serous Ovarian Neoplasms

M. Herman Chui[a,*], Qianqian Song[b], Jiarun Zhu[b], Yuchen Jiao[b], Brant Wang[c], Yeh Wang[d], Tian-Li Wang[d], Russell Vang[d,e], Ie-Ming Shih[d,e]

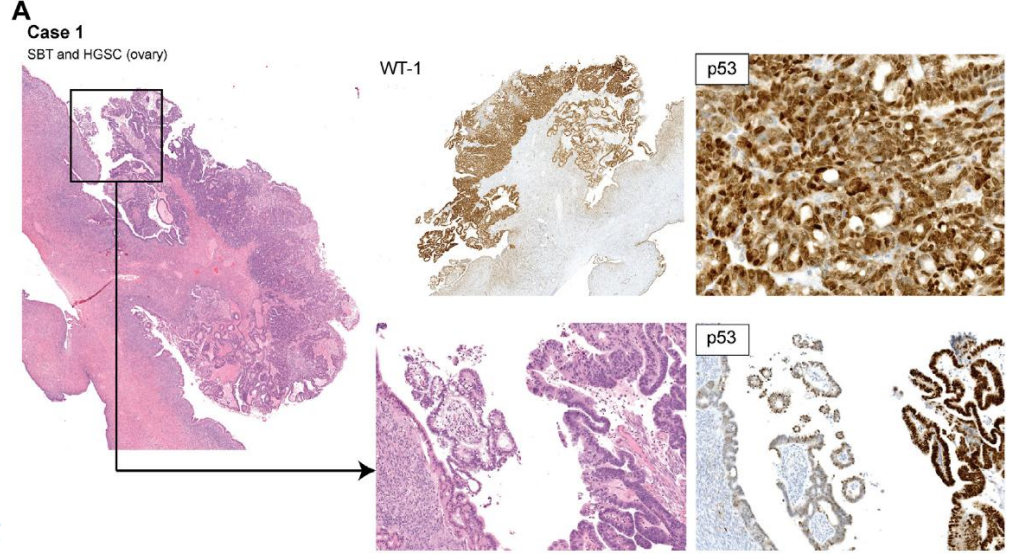

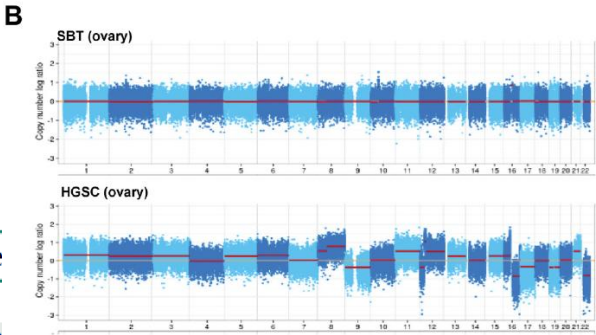

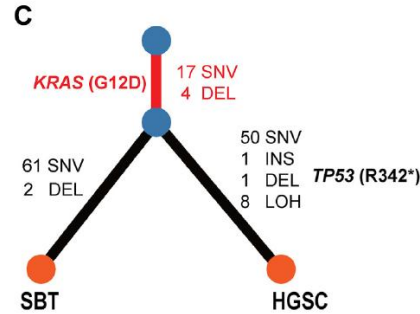

In most cases, there were relatively few somatic mutations shared between matched low-grade and higher-grade tumors compared with private mutations specific to each component (ie, phylogenetic trees with short trunks and long branches). Truncal mutations, present across all tumor samples from a given patient, included known drivers of low-grade serous neoplasms: *KRAS* (G12D, n = 4), *BRAF* (G469A, n = 1), *NF2* (n = 1), and *USP9X* (n = 1). Transformation to HGSC was associated with a *TP53* mutation

Table 1
Summary of clinical information

Case no.	Age (y)	Initial diagnosis	Stage	Clinical follow-up (from time
1	27	SBT with HGSC	I	--Lost to follow-up
2	33	SBT	I	--IGSC, peritoneal rec. (25 y) --Lost to follow-up
3	59	LGSC	III	--High-grade Mullerian carcinoma, pelvic lymph node rec. (44 mo) --Died (74 mo)
4	55	SBT with HGSC	IV	--HGSC, abdominal wall rec. (8 mo), --Alive with disease (40 mo)
5	35	miSBT (ovary) with IGSC (diaphragm)	IV	--HGSC, axillary lymph node rec. (33 mo) --Died (49 mo)
6	35	miSBT with LGSC	III	--IGSC (55 mo), peritoneal rec. --LGSC, chest wall rec. (78 mo) --Alive with disease (11 y)
7	70	SBT with LGSC	IV	--Undifferentiated sarcomatoid carcinoma rec. (37 mo) --Died (37 mo)

HGSC, high-grade serous carcinoma; IGSC, indeterminate-grade serous carcinoma; LGSC, low-grade serous carcinoma; miSBT, micropapillary serous borderline tumor; rec., recurrence; SBT, serous borderline tumor.

The British Association of Gynaecological Pathologists

Thank you!

cparra-herran@bwh.harvard.edu